AD-A074 160 JOHNS HOPKINS UNIV BALTIMORE MD SCHOOL OF ENGINEERING F/G 20/1
OPTICAL PROBING OF ACOUSTIC EMISSION WAVES.(U)
AUG 79 C H PALMER, R E GREEN DAAG29-76-G-0160
UNCLASSIFIED ARO-13666.6-MSX NL

| OF |
ADA
074160

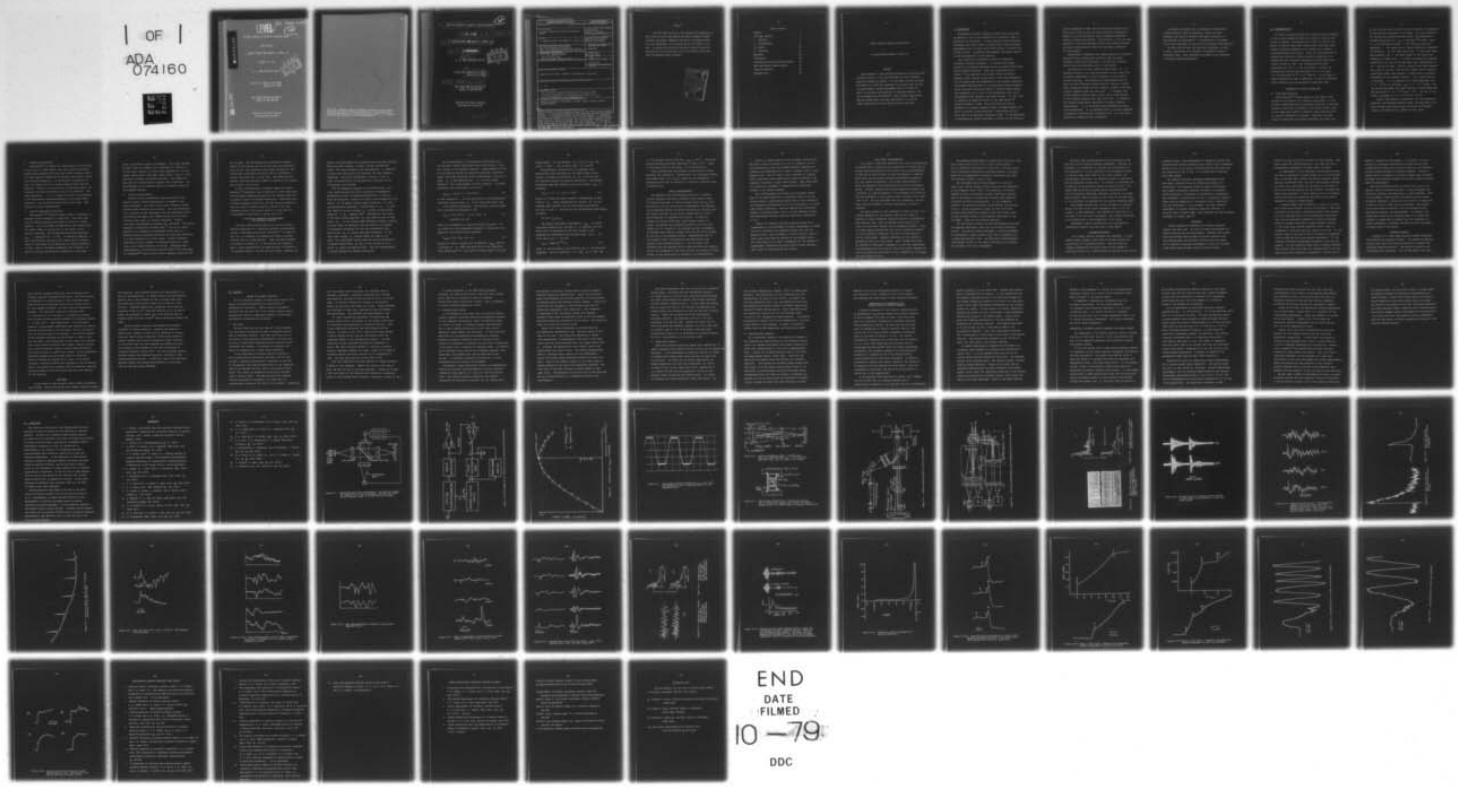

END
DATE
FILMED
10 -79
DDC

12

OPTICAL PROBING OF ACOUSTIC EMISSION WAVES

FINAL REPORT

C. HARVEY PALMER AND ROBERT E. GREEN, JR.

AUGUST 31, 1979

U. S. ARMY RESEARCH OFFICE

GRANTS No. DAAG-29-76-G-0160
DAAG-29-78-G-0050

THE JOHNS HOPKINS UNIVERSITY
SCHOOL OF ENGINEERING

The view, opinions, and/or findings contained in this report are those of the authors and should not be construed as an official Department of the Army position, policy, or decision, unless so designated by other documentation.

(6) OPTICAL PROBING OF ACOUSTIC EMISSION WAVES

(9) FINAL REPORT. 15 Feb 76-30 Jun 79

(10) C. HARVEY PALMER AND ROBERT E. GREEN, JR

(11) 31 AUGUST 1979

(12) 74p.

U. S. ARMY RESEARCH OFFICE

(15) GRANTS No. DAAG 29-76-G-0160,
DAAG 29-78-G-0050

(18) ARO (19) 13666.6-MSX

THE JOHNS HOPKINS UNIVERSITY
SCHOOL OF ENGINEERING

191 800

SECURITY CLASSIFICATION OF THIS PAGE *(When Data Entered)*

REPORT DOCUMENTATION PAGE

READ INSTRUCTIONS BEFORE COMPLETING FORM

1. REPORT NUMBER

2. GOVT ACCESSION NO.

3. RECIPIENT'S CATALOG NUMBER

4. TITLE *(and Subtitle)*
Optical Probing of Acoustic Emission Waves

5. TYPE OF REPORT & PERIOD COVERED
Final Report
2/15/76 - 6/30/79

6. PERFORMING ORG. REPORT NUMBER

7. AUTHOR(s)
C. Harvey Palmer and Robert E. Green, Jr.

8. CONTRACT OR GRANT NUMBER(s)
DAAG-29-76-G-0160
DAAG-29-78-G-0050

9. PERFORMING ORGANIZATION NAME AND ADDRESS
The Johns Hopkins University
Dept. of Electrical Engineering and of
Civil Engr./Materials Sciences and Engrg.
Baltimore, MD 21218

10. PROGRAM ELEMENT, PROJECT, TASK AREA & WORK UNIT NUMBERS
P-13666-MSX

11. CONTROLLING OFFICE NAME AND ADDRESS
U. S. Army Research Office
Post Office Box 12211
Research Triangle Park, NC 27709

12. REPORT DATE
Aug. 31, 1979

13. NUMBER OF PAGES
69

14. MONITORING AGENCY NAME & ADDRESS *(if different from Controlling Office)*

15. SECURITY CLASS. *(of this report)*
Unclassified

15a. DECLASSIFICATION/DOWNGRADING SCHEDULE

16. DISTRIBUTION STATEMENT *(of this Report)*
Approved for public release, distribution unlimited.

17. DISTRIBUTION STATEMENT *(of the abstract entered in Block 20, if different from Report)*
NA

18. SUPPLEMENTARY NOTES
The view, opinions, and/or findings contained in this report are those of the author(s) and should not be construed as an official department of the Army position, policy, or decision unless so designated by other documentation.

19. KEY WORDS *(Continue on reverse side if necessary and identify by block number)*
Acoustic emission, materials, indium, glass, steel, optics, interferometry

20. ABSTRACT *(Continue on reverse side if necessary and identify by block number)*
Optical probing is a newly developed technique for quantitative study of acoustic emission. It has great advantages over other techniques, especially piezoelectric probing: It is non-contact and does not disturb the signals, it is absolutely calibrated, has a sensitive area only tens of microns diameter, can make measurements within a millimeter of a source, can be used to probe internally in transparent materials, and has an extremely wide, flat bandwidth. With our optical probe we have measured extremely short rise times, amplitudes of 1 to 10 Å, and signals characteristic of their sources-at least in some cases.

angstroms

DD FORM 1 JAN 73 1473 EDITION OF 1 NOV 65 IS OBSOLETE

SECURITY CLASSIFICATION OF THIS PAGE (When Data Entered)

Foreword

This final report for the U.S. Army Research Office summarizes the work carried out under Grants DAAG-29-76-G-0160 and DAAG-29-78-G-0050. The authors are greatly indebted to both the U.S. Army Research Office and to Dr. George Mayer, their technical monitor, for support in this work. The authors feel that optical probing of acoustic emission has been shown not only to be possible, but to yield superior results which cannot be obtained be other techniques.

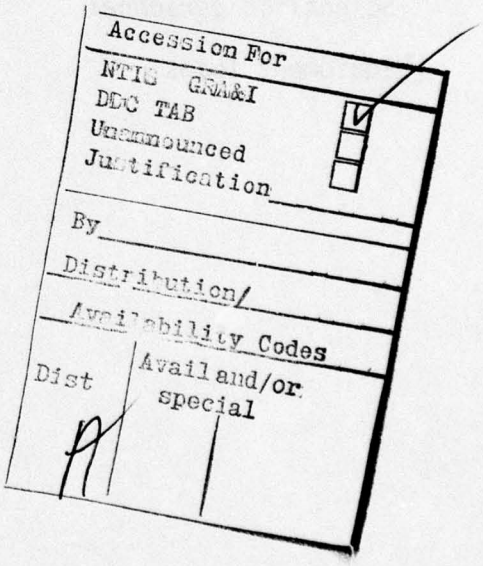

Table of Contents

Optical Probing of Acoustic Emission Waves

C. Harvey Palmer and Robert E. Green, Jr.

ABSTRACT

Optical probing is a newly developed technique for quantitative study of acoustic emission. It has great advantages over other techniques, especially piezoelectric probing: It is non-contact and does not disturb the signals, it is absolutely calibrated, has a sensitive area only tens of microns diameter, can make measurements within a millimeter of a source, can be used to probe internally in transparent materials, and has an extremely wide, flat bandwidth. With our optical probe we have measured extremely short rise times, amplitudes of 1 to 10 Å, and signals characteristic of their sources-at least in some cases.

I. OBJECTIVES

Transducer generated ultrasonic pulses have long played an important role in the nondestructive evaluation (NDE) of materials and structures. In the pulse-echo and pitch-catch techniques the travel times of pulses serve to make thickness measurements and to locate flaws which scatter or reflect the acoustic pulses. Attenuation measurements can detect changes in the microstructure of the material.

More recently an alternative method for materials evaluation has been developed. It involves the passive detection of naturally generated bursts of elastic wave energy called acoustic emission. Since the pioneering work of Kaiser,[1,2] who made the first careful study of acoustic emission from a variety of materials, it has been speculated that the amplitudes and frequencies of the acoustic emissions are somehow characteristic of the generating source mechanism (slip, twinning, dislocation motion, cracking, phase change, void formation, etc.), and, of the propagation path, and of the specimen size, geometry, and state as well. If true, this is certainly an important factor in the application of acoustic emission to NDE. We do know that the rate of generation of acoustic emission bursts increases rapidly just prior to failure in many materials. Thus monitoring the burst rate is an important technique of NDE. If the hypothesis of characteristic signal waveforms is valid, the monitoring of

acoustic emission for NDE could be much more valuable for we would then be able to use the burst waveforms to determine whether or not the particular bursts represented harmless events or deleterious effects. Unfortunately, it has not been possible to test this hypothesis until very recently because the usual (piezoelectric) sensor is completely inadequate for the purpose.

Piezoelectric transducers are indeed sensitive to acoustic emission bursts (perhaps more sensitive than any other transducer under some conditions), but they have grevious faults which are documented later in this report.

The objectives of this research program were: (1) to determine whether or not optical methods, so very useful for ultrasonic measurements, could be adapted to the study of acoustic emission. We believed that such methods could be used, but the differences between regular, periodic, narrow band, ultrasonic pulses and the irregular, random, broad-band acoustic emission waves are very great. (2) assuming that optical methods could be made to work (and we were assured at one technical meeting that they would not!), to determine the detailed quantitative waveforms of acoustic emission displacements. (3) to correlate these waveforms with their source mechanisms. (4) to determine what is actually measured by commercial piezoelectric transducers and (5) to provide a method for calibrating such transducers.

To achieve our objectives, we proposed to investigate various potential optical techniques, select the most promising one, build a suitable instrument, optimize it, and evaluate its performance. If satisfactory, we planned to use this instrument to carry out our proposed investigations.

We feel that our work has been very successful; we have, in fact, constructed four different instruments suited to different tasks. Each instrument has added to our knowledge of acoustic emission phenomena.

II. INSTRUMENTATION

To design an optical system for acoustic emission research, we had to make assumptions about the nature of what we were trying to measure. We assumed that a burst or "event" is a packet of elastic waves which arise within a material under stress and which propagates on the surface as a radially spreading Rayleigh wave group. Given the characteristics of commercially available acoustic emission transducers, we assumed that the principal frequencies involved range from roughly 20 KHz to 2 MHz. The corresponding Rayleigh wavelengths are 140 to 1.4 mm on aluminum. Further, we supposed that typical wave amplitudes lie in the range 1 to 100 Angstroms (10^{-10} to 10^{-8} meters). On the basis of these assumptions we made a comparison of optical techniques before selecting the interferometric techniques used.

COMPARISON OF OPTICAL TECHNIQUES

A. Knife-edge Technique

This technique[3,4] senses changes in the slope of the surface of the material as a Rayleigh wave passes. It can be used to determine both the amplitude and phase of the wave. Ideally a laser beam is focused on the surface using a lens of the right focal length to produce a spot size just half an acoustic wavelength in diameter. Obviously the wide range of wavelengths anticipated precludes this ideal size,

so that we would have to make the spot size small in comparison to the shortest wavelength to be sensed. For this situation, the theoretical minimum detectable angle (corresponding to maximum sensitivity) is $\theta_{min} = (2eB/\alpha P_0)^{1/2} D/(2\sqrt{2}f)$. Here e is the electronic charge, B the effective amplifier bandwidth, α the sensitivity of the photodetector (amps/watt of radiation), P_0 the laser beam power, D the input laser beam diameter, and f the focal length of the input lens. Evidently we should make D as small as possible for maximum sensitivity, but then the focused spot size, proportional to f/D, may be too large. Taking a typical laser beam diameter as 1.6 mm, we can use a 200 mm focal length lens to obtain a sufficiently small spot diameter - roughly half an acoustic wavelength for the highest frequency. For a laser power of 1 milliwatt, $\alpha = 0.42$ amp/watt for a good photodiode, and $B = 2 \times 10^6$ Hz, we calculate $\theta_{min} = 1.1 \times 10^{-7}$ radian. For the 140 mm wavelength this angle implies a minimum detectable wave amplitude of 2.5×10^{-6} mm or 25 Å. For the 1.4 mm waves, the height is 2.5×10^{-8} mm or 0.25 Å.

Clearly this method is insensitive for low frequencies. Moreover, the technique measures slope, not amplitude, so we must integrate the output signal to obtain the waveform. Finally, the method is not useful for bulk waves.

B. Diffraction Technique

This method[4-9] is useful for either surface or bulk waves. A long train of elastic waves acts like a phase diffraction grating which scatters the light into various spectral orders. If a wide range of frequencies is present, the spectral orders will be widely spread out. If the acoustic wavelengths are long, the orders will be so crowded together they cannot be measured. Finally, if the wave train is relatively short, the "grating" will have insufficient lines to be effective. The order separation, $\theta = \lambda/\Lambda$, would vary from 4.5 microradians to 450 microradians making measurement of the orders almost impossible. The intensities would also be very weak. This method is clearly unsatisfactory.

C. Optical Heterodyning Technique

This method,[4,10] used for surface waves, is dependent on frequency shifts produced by a Bragg cell. The laser beam and the frequency shifted laser beam are mixed in a photodetector. One of the beams is modulated by the acoustic wave. The output signal is proportional to the square of the acoustic amplitude. The minimum detectable wave amplitude, $\delta_{min} = (2eB/\alpha P_0)^{1/2}\lambda/\Lambda = 0.10\mathring{A}$, is certainly adequate. A major difficulty is that since the output signal is proportional to the square of the amplitude, all phase information is lost. Even if the phase information were available, we could not extract the amplitude information in real time

since the electronic speed is inadequate. The Analog Devices IC Model 436B, for example, has a bandwidth of 1 MHz for a 10 volt input signals, but only 30 KHz bandwidth for .01 volt inputs, which gives a very small useful range. Thus it is not practical to display the desired waveform. The method has been used for visualization of surface wave intensities. The disadvantages of the technique made it of doubtful value for the proposed research.

D. Optical Interferometry

Since two beam interferometry measures directly the quantity sought, surface displacement, it seemed to have great advantages. Our previous work with ultrasonic surface and bulk waves suggested this solution. The chief difficulty to be overcome was the requirement that the pathlength difference between the sample and reference paths had to be held constant within about 0.1 optical wavelength. Several alternative interferometric methods were considered. Our earlier technique, differential interferometry,[11] was not an option because it is intended for measurements where there is a definite acoustic wavelength and where the waves are travelling in a known direction (in either sense). Acoustic emission obviously involves a number of wavelengths spanning a large range, and a random direction of arrival. Quadrature dual interferometry, an invention of Peck and Obetz[12] and later used by Vilkomerson[13] uses two polarization components which are 90°

out of phase. The two photocurrent signals are squared, added, and the square root of the sum taken electronically. First of all, this technique looses phase information, and sufficiently high speed electronics was not available to extract the square root in real time. The technique does, however, make the instrument immune to changes in one optical path relative to the other.

A third interferometric technique, swept path interferometry,[14] guarantees that at some point in the sweep cycle that the phase difference between the two optical paths will be exactly correct for maximum sensitivity. Aside from loss of phase information here also, the most serious problem is that the acoustic emission signal is likely to be lost altogether since it may easily arrive at a time when the interferometer sensitivity is either low or nil.

A PRACTICAL MICHELSON INTERFEROMETER FOR ACOUSTIC EMISSION

The first optical probe used in our earlier acoustic emission experiments is a modified Michelson interferometer having a stabilized optical path difference.[15] As shown in Fig. II-1, an expanded, collimated laser beam is incident from the left on a beam splitter. Light reflected downward is focused on a mirror at P and provides the reference path. Light transmitted by the beam splitter is focused on the specimen surface. The two returning beams, reference and

sample, are recollimated and superposed above the beam splitter, where they form (ideally) a single, uniform interference fringe. The light focused on the photodetector, D , generates a photocurrent having both low frequency and high frequency components. The signal frequencies, typically 10 KHz to 1 MHz, are amplified by the RF amplifier, displayed on the oscilloscope, and recorded.

The low frequency component of the photocurrent, 0 to 1 KHz, which results from room vibrations and atmospheric disturbances as well as specimen deformations, is used to drive the stablizer. Figure II-2 shows a block diagram of this system. At the desired optical phase difference, $\pi/2 \pm 2N\pi$, the photodetector generates a voltage equal to E_r . In this case there is no error voltage E_e , and the voltage across capacitor C , E_c , remains fixed. Consequently, the output of the high voltage amplifier E_0 also remains fixed as does mirror M_2 . If the optical phase difference changes, however, an error signal is generated, and the capacitor is charged or discharged accordingly so that the piezoelectric unit moves mirror M_2 to correct the phase difference. In the event that voltage E_0 becomes either too large or too small, the "over-under" switch opens the circuit momentarily to permit moving mirror M_2 one or more fringes so as to bring E_0 within the desired range. Thus the interferometer is always adjusted for maximum sensitivity.

The interferometer is calibrated by substituting for the specimen a second piezoelectrically driven mirror. This unit, driven at its resonant frequency - approximately 140 KHz - by a variable RF voltage of sufficient amplitude, provides a large, controlled sinusoidal mirror displacement, $\delta=\delta_0 \cos \omega_a t$, where δ_0 is the amplitude and ω_a is the RF radian frequency. For a displacement from the quiescent $\pi/2$ phase difference, the photocurrent is given by

$$i_{photo} = (\alpha P_i/2) \; [1 - \sin(4\pi\delta/\lambda)] \; . \qquad (1)$$

In this expression, α is the sensitivity of the photodetector (amps/watt optical power), P_i is the laser beam power, and λ is the optical wavelength. The amplifier output voltage for a sinusoidal disturbance is then

$$V_{out} = K \sin [(4\pi/\lambda) \; \delta_0 \cos (\omega_a t)] \quad \text{or} \qquad (2)$$

$$= K_1 \sin(K_2 \cos \omega_a t) \; ,$$

which can be expanded in a series of Bessel functions. If we include only the fundamental frequency, filtering out the harmonics, the voltage can be expressed

$$V_{fund} = 2K_1 \; J_1(K_2) \cos \; \omega_a t \; . \qquad (3)$$

Figure II-3 shows a typical plot of measured V_{fund} data as a function of δ_0 where the solid line is the theoretical curve proportional to $J_1(X)$ which has been scaled to fit the

maximum point. At this maximum, $K_2 = 4\pi\delta_0/\lambda = 1.84$ and $J_1(K_2) = 0.5812$. For our He-Ne laser $\delta_0 = 926.6\text{Å}$.

Alternatively, and better for our purposes, with sufficiently large disturbances, the peak-to-peak output voltage, including all harmonics, is $2K$ so that we have the required constant for absolute calibration. The minimum disturbance amplitude needed to give this voltage, v_{cal}, is evidently

$$4\pi\delta_0/\lambda = \pi/2 \quad \text{or} \quad \delta_0=\lambda/8 = 791\text{Å} . \tag{4}$$

Figure II-4 shows the signal waveform corresponding to this value of δ_0 . Having determined the constant $2K$, we now consider small signals, and for this purpose approximate sin x by x in Eq. 2. Solving for the instantaneous displacement, we obtain

$$\delta=(\lambda/2\pi)\ v_{out}/V_{cal} . \tag{5}$$

The minimum detectable displacement, δ_{min} , is easily calculated theoretically (see Ref. 4) by observing that the noise level is determined by the shot current in the photodetector generated by the constant power $\alpha P_i/2$, the first term in Eq. 1. We find

$$\delta_{min} = (2eB/\alpha P_i)^{1/2}\lambda/4\pi , \tag{6}$$

where e is the charge on the electron, and B the amplifier bandwidth. For our instrument, $B = 1$ MHz , $P_i = 1$ mW , and

α = 0.4 amp/watt, and we find that δ_{min} = 0.04 Å . The actual measured minimum detectable amplitude is about 1/2 Å . (Most of the noise arises in the laser, not in the detector.)

This interferometer has yielded, and continues to yield, important new information. Nevertheless, the instrument suffers from undue sensitivity to room vibrations and atmospheric disturbances and must be mounted on a vibration isolation table to perform well.

FIZEAU INTERFEROMETER

We designed a new interferometer primarily to measure acoustic emission from small specimens during tensile tests. Our intention was also to obtain a design which was far less sensitive to the room vibrations and atmospheric disturbances. In the Michelson design, torsional vibrations of the base plate were easily excited, and an in-line design based on Fizeau optics promised to eliminate that problem. In addition, because the optical paths have a much greater portion in common, we expected the atmospheric effects to be much less. Figure II-5 is a diagram of the improved optical arrangement. An expanded laser beam is incident from the left and is focused by the lens on the specimen surface. Approximately half of the incident light is reflected by the beam splitter and focused on the reference mirror R . The two beams, one reflected from the specimen and one reflected from the reference mirror, are recombined at the beam splitter and produce a fringe pattern at the output which is focused on the photodetector.

Figure II-6 shows details of the reference mirror drive. The mirror itself is mounted on a 1/8 in. diameter, 1/2 in. long piezoelectric tube and provides possible correction of vibrations with amplitude up to about 6 fringes, with a 1 msec response time. The PZT tube in turn is mounted on a spring steel strip which can be magnetically moved to provide a low frequency correction of about 6000 fringes. This large range of correction is designed to compensate for dimensional changes in the tensile specimen.

This interferometer has proven to be unusually stable. When it is placed directly on a laboratory bench or on the tensile machine, random fringe motion due to room vibrations and atmospheric disturbances is not more than about 0.1 fringe under normal conditions. Thus the required path correction needed is relatively small, and it is even possible to make some measurements without using the correction electronics at all.

Figure II-7 shows an auxiliary viewing system to be incorporated in the instrument to permit photography or closed circuit TV viewing of the specimen surface very near the measured point. The two plates, P1 and P2 cause no loss of laser light since they are mounted at the Brewster angle. The first plate, P1 is used to compensate for the transverse displacement produced by the thick plate P2 which reflects white light to the microscope for viewing.

DUAL PROBE INTERFEROMETER

As a result of the data obtained by our first interferometer, we decided that it would be very informative if we were able to record accurate waveforms at two or more points simultaneously. In this way we would be able to study the changes in waveform which occur as the acoustic emission disturbance propagates. For this purpose we designed a dual probe interferometer in which the spacing of the probing points could be continuously varied. Further, because the waveform apparently changed over a distance of a few millimeters, it was necessary to be able to vary the separation of the probing points from zero to at least 15 mm or so. The new instrument has this capability, and the range could be extended to several centimeters or more if required.

The basic optics of this instrument is shown in Fig. II-8. Primary separation of the signals from the two probes is achieved by using orthogonal polarizations with a polarization beam splitter cube. This arrangement directs most of the light for each probe through its own respective channel. Since the light passing through the cube is not collimated, however, it is not perfectly separated, and there is some mixing of the two light beams. Complete separation of the signals is achieved by the use of two lasers. Their frequencies differ by hundreds or thousands of megahertz so that any interference patterns between the two slightly mixed light beams averages out over the relatively restricted (10 MHz) bandwidth of our system and thus causes no error.

The desired probe spacing is achieved by sliding the lower unit (lower right of Fig. II-8, in box) either right or left to translate probe point P2 vertically. The lower probe can be focused by adjusting the specimen position; the upper probe can be independently focused by translating the upper unit (boxed in figure) right or left.

The instrument has not been assembled in its final form as yet, partly because we must allow for the dimensions of the permanent laser (still to be acquired), and partly because we wish to incorporate several additional features, such as the ability to adjust the relative probe positions vertically as well as horizontally. (In the temporary mounting, the horizontal spacing is adjustable, the vertical is not.) As the instrument is used, we will find other features which should be included in the final model, such as more flexible control of the relative directions of the two beams. (They are now strictly parallel.)

The electronic circuitry for the interferometer involves two separate amplifiers, each with its own path correction control. As with the second instrument, it may be desirable to incorporate a larger control range than is possible with a single piezoelectric tube. The additional electromagnetic (slow speed) control of the second instrument will probably be included in the final arrangement.

The dual probe interferometer can be calibrated in the same way as the original Michelson instrument. Although, in principle, it is possible to calculate the calibration for the instrument, it is not practical to do so because we need to know the laser light level in the fringe pattern, the photodetector sensitivity (in amperes per watt of radiation), and the amplifier voltage gain. It is better to determine the calibration by continuously varying the optical path in the sample beam by driving a sample mirror piezoelectrically with an adjustable amplitude sinusoidal voltage at a suitable high frequency (about 100 KHz, in the center of the pass band of our amplifier) as described for the earlier Michelson model.

The ultimate sensitivity of this instrument is slightly better than that of the first instrument, about 0.5 Å for roughly a 10 MHz bandwidth. The theoretical sensitivity is the same as for the other instruments. The primary limitation in our sensitivity is the instability of our lasers.

Preliminary results obtained with this instrument as termporarily mounted are given later in the report.

ALTERNATIVE METHODS

A far simpler optical technique was attempted. In this method a small diameter laser beam is directed through the sound field in a transparent medium. The laser beam is slightly deflected by the sound field and the change in positions relative to a fixed pinhole is detected by the optical

intensity change. This arrangement is capable of sensing both ultrasonic and acoustic emission sound fields within transparent medium, but it is not easy to calibrate and has been used only as a qualitative tool so far. It is effectively a modified knife edge method.

Yet another technique, developed independently from this Grant, provides true three dimensional probing of a sound field. The technique, based on Doppler velocimetry, has yielded interesting transducer patterns of ultrasonic fields generated in plexiglass by piezoelectric transducers. This technique is quantitative and can, in principle, measure three velocity components of the partial motion associated with the sound field. It is probably less well suited to measurement of acoustic emission transients although it should be able to detect them. This technique has been partially described in a short paper.[16]

RECORDING

Several methods for recording our acoustic emission signals have been used. At first we simply photographed the traces directly from the oscilloscope. Although some signals were lost because they occurred during the retrace of the oscilloscope beam, the principal objection was that there was no suitable triggering arrangement to blank out the many traces which occur between acoustic emission events.

Figure II-9 shows one of the earliest of these signals. The upper signal was obtained optically, the lower one with a piezoelectric transducer; the sweep speed 1 msec/div.

An improvement in this technique could be made by using the event to generated a trigger signal for the oscilloscope and, at the same time, passing the acoustic emission signal through a broad-band delay line which would permit recording the noise level just before the occurrence of the event as well as the initial features of the waveform. Although this method seems excellent, it does require the use of suitable delay lines which are expensive and which are not easily adjusted to produce suitable delays.

A better method, used extensively in much of our work, was a video tape recorder (or pair of recorders). With such a recorder one can make a continuous record of the signals and later play them back on the oscilloscope screen where they can be conveniently expanded or shifted as desired. There are several objections to this technique, however: (1) The video tape recorder bandwidth, about 4 MHz, is inadequate to study the important initial rise time. (2) The dynamic range of the tape is far too limited to accommodate both the weak and the strong signals encountered. (3) The recorder introduces considerable extraneous noise into the signals. (4) The recording format used in readily available VTRs involves dead time, when the recording head is off the tape during which recording is impossible. We have lost a

number of signals for this reason. (5) Finally, it is not possible to correlate accurately two signals such as from a piezoelectric sensor and an optical sensor or two different optical signals recorded on different machines. (Pairs of signals must be recorded on two single channel tape recorders and small time intervals between the acoustic emission signals cannot be determined.)

The best recording method, we found, was to use a two channel, digital transient recorder, a Nicolet Explorer III, having two channels and effectively a 10 MHz bandwidth. With this instrument, which provides mid-signal and post signal triggering capability, signals can be stored on a floppy disk in digital form for later recall and display. The signals can be positioned as desired on the oscilloscope screen, magnified as desired, and photographed. In addition, the floppy disk signal may be recorded either on an analog X-Y recorder or transmitted in digital form to a computer for further processing. Waveforms recorded with this instrument are shown later in the report.

SPECTRAL ANALYSIS

A number of our video taped acoustic emission waveforms were analyzed for frequency content. Two methods of spectral analysis were used; Fast Fourier Transform by computer and electronic spectrum analyzer. The results obtained by the two methods were comparable. For the FFT method, the video

taped signals, properly identified, were digitized with a transient recorder (Biomation Model 8100). The VTR recording was examined on an oscilloscope to find a suitable frame. Using the gated oscilloscope output as the trigger source for the transient recorder, the event could be captured for analysis. Two digitizing rates were initially used: 0.2 μsec.point and 0.5 μsec/point. By Nyquist's theorem, this provided accurate spectral analysis for frequency ranges 0 - 2.5 MHz and 0 - 1 MHz respectively. For the signals examined, no appreciable differences were observed for spectra obtained by digitizing at the two rates. The 0.5 μsec/point rate was used for most of the analyses. The storage capacity of the transient digitizer was 2048 points so that, at this rate, the first 1.024 milliseconds of each signal was analyzed. Both a Fast Fourier Transform (FFT) digital computer program and a spectrum analyzer (Hewlett Packard Model 8552/8553A) were used initially to examine the signals. Little significant difference between the two methods could be discerned. Figure II-10 shows the spectra for an event in the stress corrosion cracking of E4340 steel obtained by the two methods. Most of the signals were analyzed with the commercial spectrum analyzer because it was much faster than using the computer for the analysis.

SPECIMENS

In the course of this research various kinds of specimens were studied. Both simulated and real acoustic emission signals

were measured. The simulated signals were used primarily to test our instrumentation, to compare optical and piezoelectric sensors, and to test theories of what a surface step pulse and buried step pulse signal looked like as seen by a fast detector. Simulated signals were generated either with the technique of Hsu et al[17] using the breaking of 1/2 mm lead on either the proximate or remote side of an aluminum disk or breaking glass capillary tubing[18] which yielded more abrupt rise times.

Natural acoustic emission was generated by suitable stressing of various materials. Twinning was induced by bending zinc, cadmium, indium, and tin specimens of various sizes and under various conditions; cracking was induced in glass by thermal means and also mechanical means; cracking in both E4340 steel and 7039 aluminum was induced by stress and corrosion; phase changes in iron wire was induced by electrical heating to about 900°C. All the resulting acoustic emission signals were measured optically, and some of them piezoelectrically as well. In addition, some of the optically detected signals were probed simultaneously at two points with our new dual probe instrument.

III. RESULTS

NATURE OF ACOUSTIC EMISSION

We have obtained a number of results which bear on the nature of acoustic emission and its applications to nondestructive evaluation. These results are concerned primarily with the rise time of an acoustic emission burst, propagational effects, temperature effects, and the basic hypothesis of characteristic waveforms.

A. Rise Time

We have found that the rise time of a burst measured near the source is probably an order of magnitude shorter than is generally observed. This very fast rise time is, we believe, a most important characteristic of bursts and may help to distinguish different acoustic emission source mechanisms and, perhaps, to determine the distance from source to transducer for a known source mechanism.

In our experiments on stress corrosion cracking in heat treated E4340 notched steel specimens (18×17×75 mm), we used a commercial piezoelectric transducer on the side of the specimen and probed optically both on the (opposite) side of the specimen and very close to the growing crack. Figure III-1 shows two successive bursts which occurred about 4 millisec apart. The upper waveform was obtained with the piezoelectric transducer, the lower with our interferometer probing at the side of the specimen. Considering

that the sensors were 18 mm apart, the waveforms are in reasonable agreement. Frequency components up to 500 KHz were observed, with most of the activity in the 0 to 100 KHz range. We found no significant changes in the spectral content as the crack grew longer and longer. These waveforms were recorded on video tape, displayed on the oscilloscope and photographed. The bandwidth was approximately 4 MHz.

In a more interesting experiment, we positioned the optical probe within a millimeter of the growing crack while not disturbing the piezoelectric transducer position. Then a very significant difference was found between the two signals. As shown in Fig. III-2, the optical signal showed a strong, abrupt initial step for both bursts which was completely absent in the piezoelectric signals. For this experiment we then increased the amplifier bandwidth to about 5 MHz used a Nicolet Explorer II transient digitizer having a frequency response to 10 MHz. Figure III-3 shows an unusually abrupt rise which occurred in 1/5 microsecond or less. The step amplitude was of the order of 10Å.

Fast rise times have also been observed in stress-corrosion cracking of 7039 aluminum. Figure III-4 shows a rise time of about the same as that in the steel specimen. Figure III-5 shows a 200 μsec record of the aluminum which reveals an interesting series of short bursts which occurred at intervals of about 40 μsec.

In indium specimens at low temperatures emission generated by twinning also shows a fast rise time, though not as fast as for cracking of steel or aluminum. Figure III-6 shows a rise time of about 1 μsec in specimens at liquid nitrogen temperature, -190°C.

B. Propagational Effects

It was assumed at the outset that, for several reasons, acoustic emission waveforms change with propagation distance. (1) The component dilatational, shear, and Rayleigh waves of a burst all travel at different speeds. Most materials are at least slightly anisotropic so that there will be additional speed changes with direction. (2) The burst wave amplitude will be attenuated with propagation distance because of geometric spreading from an isotropic source directly in proportion to distance for bulk waves, proportional to the square root of distance for Rayleigh waves. In addition, since attenuation also results from frequency dependent loss mechanisms, the waveform will also be modified on this account. (3) Specimen resonances, reflections, and mode conversions also will modify the waveforms.

Preliminary, rather qualitative evidence of propagational effects was obtained from measurements of stress corrosion cracking in steel made at 1,2, and 10 mm from the growing crack. The highest frequency components were rapidly attenuated with distance as expected, but the results were

poor because, with only a single probe, we had to compare different bursts not exactly alike. Later, using our dual probe interferometer and a Nicolet Explorer III oscilloscope, we obtained better data showing waveform changes. Figure III-7 illustrates the agreement of data obtained with the two probes when superposed (zero separation). The difference in amplitude of the two signals results from somewhat different laser power and amplifier gains in the two channels. (The path correction electronics was not used.) The horizontal scale is 25 μsec for the whole trace.

Figure III-8 shows differences in waveform when the two probes were separated by 1 mm. The total sweep in this case was 102 μsec. The bursts were generated in indium (room temperature) and measurements made about 10 mm (lower trace) from the twinning source and 11 mm (upper trace) from it. Although the waveforms are very similar, they do not differ merely by a scale factor. The various propagational effects, mentioned above, account for the differences. Figure III-9 shows indium waveforms obtained at points 5 mm apart. Some of the harmonic content in the lower trace is greatly reduced by the extra 5 mm propagation distance. The later part of the lower waveform is nearly absent in the upper trace. (Unfortunately the initial part of the waveforms was not recorded because of a triggering problem in the oscilloscope.)

Dual probe experiments were also carried out in thermally cracked glass. The probe beam was transmitted through a 1/4" glass plate to a mirror which returned the beam through the glass (thus doubling the optical path changes resulting from the acoustic emission waves.) In most cases the signals were so large that even at very low gain the amplifier was usually driven into saturation so that the data was virtually useless. Figure III-10 shows two of the satisfactory waveforms obtained. The separation was 10 mm, the full horizontal trace was 102 μsec. Because the exact site of crack initiation was somewhat uncertain, we do not know that one acoustic path is just 10 mm greater than the other. Propagational effects on the waveforms are certainly present, but their interpretation is not entirely clear.

C. Temperature Effects

Since many material properties depend upon temperature, it seemed reasonable that acoustic emission would also be temperature dependent. In our experiments we measured twinning in indium at temperatures ranging from liquid nitrogen to nearly the melting point. We found that at higher temperatures the higher frequencies were much less pronounced. At -190°C, as shown in Fig. III-11 (upper two traces) frequencies of up to about 200 kHz could be observed at the end of the specimen (about 10 mm from the twinning site). At +100°C we observed much lower frequencies (lower two traces). At

still higher temperatures, roughly 120°C, no bursts were detected. This observation is not unexpected since the melting point of indium is only +155°C. We expect that for other materials, zinc, tin, and cadmium we would find the cessation of acoustic emission at higher temperatures because of higher melting points. These experiments were not carried out since we did not have suitable small (1/8×1/8×1 1/2") specimens of these materials. It would be interesting to measure the cut-off temperatures: Are they rather abrupt or very gradual? Is there a correlation between some cut-off temperature and the melting point?

D. Characteristic Waveform

As a preliminary answer to the question of whether or not waveforms are characteristic of the acoustic emission source, we compared the signals from indium twinning with those from a phase change in iron wire at approximately 900°C. Figure III-12 shows twinning signals (left side) and phase change signals (right side). Note that the upper pairs of signals from both sources are virtually identical. Even though the twinning signals differ from each other, as do the phase change signals, there is no difficulty in distinguishing twinning from phase change. Considerable more work needs to be done to establish the details, but we can assert that the hypothesis of characteristic signals now does have some supporting evidence.

Whether or not we can distinguish twinning in indium from twinning in zinc, cadmium or tin is less certain. The waveforms look much alike in their essential features.

COMPARISON OF PIEZOELECTRIC AND OPTICAL ACOUSTIC EMISSION SENSORS

A complete discussion of the relative characteristics of piezoelectric and optical sensors for acoustic emission is given elsewhere.[19] As shown in Figs. III-8 and III-9, there are significant differences in waveform resulting from propagational effects. We also know that the wide range of frequencies in acoustic emission signals, less than 20 kHz to at least 10 MHz, encompases a wavelength range of the order of 300 mm to 0.5 mm. The typical piezoelectric transducer has a sensitive area of diameter 12.5 to 25 mm, much larger than the shortest acoustic wavelengths and much smaller than the largest wavelengths. Furthermore, the frequency response of the piezoelectric transducer is inadequate, and it is characterized by various mechanical or electrical resonances. In addition, piezoelectric sensors are tightly coupled to the surface to be measured (and thus disturb the sound waves), cannot be independently calibrated, and cannot be used directly at either high or low temperatures.

In an experiment with cast bars of indium, zinc, cadmium and tin 150×25×6 mm, we recorded waveforms with a piezoelectric transducer on one side and with our interferometer,

directly opposite, on the other side. Twinning was induced about 50 mm away from the sensors. It was assumed that the two acoustic waveforms would be very much alike except for the highest frequencies because of the small 6 mm separation. Figure III-13 shows the observed differences in the twinning signals for indium. In both signals the higher frequencies dominate the initial 50 μsec of the burst; these frequencies persist much longer in the optical signal. Figure III-14 shows the frequency differences in the two waveforms as determined by a spectrum analyzer. Both spectra have peaks at 22 and 30 kHz, but the 22 kHz peak is weak in the piezoelectric spectrum. Also, the piezoelectric spectrum has a strong peak at 13 kHz which is very weak in the optical spectrum. The piezoelectric response at near 100 kHz is small, but very clear in the optical spectrum.

In another experiment we compared the waveforms of an ultrasonic pulse measured by a medical-type piezoelectric sensor with a 2 1/2 mm diameter axial hole and by our optical probe directed through the axial hole. The specimen surface as an aluminum block. The acoustic signals, ideally, would be almost identical. Figure III-15 shows the two observed waveforms which are quite different; the optical signal (upper trace) has significant amplitude in the regions where the piezoelectric transducer signal (lower trace) has gaps or very small amplitude. Below is the power spectrum

showing a large component at 350 kHz in the piezoelectric transducer signals, an artifact of the transducer itself, which is absent in the optical signal.

To summarize, piezoelectric transducers have the following limitations: (1) too narrow bandwidth, (2) mechanical and electrical resonances, (3) too large a sensitive area, (4) require the use of a couplant, (5) can be used only over a limited temperature range, and (6) cannot be properly calibrated. Our optical transducer has none of these limitations.

COMPARISON OF NATURAL ACOUSTIC EMISSION AND SEISMIC THEORY

Our experiments on the initial spike for stress corrosion cracking in both steel (see Fig. III-2) and aluminum (see Fig. III-4) suggested comparison with theoretical signals from seismic pulses.

If only the initial part of the acoustic emission signals is considered, we can ignore specimen resonances, reflections, and mode conversions. We treated three special cases in which the theory is tractable and which are convenient for experimental tests. The three cases involve (1) the seismic surface pulse (a semi-infinite elastic half space with excitation and sensor located on the surface, (2) the seismic buried pulse (a semi-infinite half space with the excitation below the surface sensor on a line normal to the surface through the sensor), and (3) the thick slab with sensor on

one surface and excitation directly opposite on the other surface (the slab has infinite area and a finite thickness). In each case the excitation is assumed to be a Heavyside stress step with zero rise time applied in a direction normal to the surface of the specimen.

For our experiments we used three optically polished aluminum blocks: (1) 127×127×83 mm, (2) 153 mm dia×64 mm thick, and (3) 153 mm dia×25 mm thick. The only satisfactory pulses we could generate were obtained by breaking glass capillary tubing using the method of Breckenridge et al.[18] The capillary tubes were 25.4 mm long with O.D. 0.49 mm and I.D. 0.33 mm. With a suitable mechanical mounting, we could break the glass with a micrometer pushing a pointed end. This method, according to Breckenridge et al generates pulses with a rise time of less than 0.1 μsec, very small in comparison with the travel time of the fastest wave from the excitation point to the sensor, distances of 10, 20, and 30 mm for our surface pulse measurements. According to Knopoff,[20] the mathematical model applies under these conditions.

Figure III-16 shows the theoretical surface displacement for a surface seismic pulse (Pekeris[21]). The arrival times for the P,S, and R waves are indicated. We made experimental measurements with the breaking glass excitation and obtained displacement measurements shown in Fig. III-17, III-18, and III-19 corresponding to source-sensor distances of 10, 20, and 30 mm respectively. The qualitative agreement is good.

Obviously we could not record the zero rise time step corresponding to the arrival of the Rayleigh wave because the excitation is not a true step function and also our detection electronics does not have infinite bandwidth. We believe the results obtained are reasonable, however.

Figure III-20 shows the theoretical surface displacement for a buried pulse. Figure III-21 is a recording of the corresponding measurement. Again the agreement is as good as we could expect. Finally, Fig. III-22 shows the theoretical surface displacement for the thick slab and Fig. III-23 the experimental result.

Figures III-24 and III-25 illustrate the long term behavior for the seismic buried pulse and thick slab experiments respectively. In both cases oscillations of relatively low frequency result and it is very difficult to give an adequate explanation of the behavior. Factors such as spread of the acoustic beam and high frequency attenuation surely affect the results. Also, the finite transverse dimensions of the specimen will cause edge reflections to occur and thus modify the surface displacements. These oscillations are also observed in real acoustic emission signals from all sources and are dependent upon specimen size and geometry as well as other factors mentioned.

We have made a number of measurements of bursts in stress corrosion cracking and have obtained a variety of waveforms. It can be stated in general that if the probing is done near

the growing crack, the rise time is short. In many cases the signals resemble the theoretical displacements for seismic pulses. Figure III-26 shows some of the typical bursts observed in steel with typical short rise times. All bursts do not behave in this way; doubtless reflections and other phenomena modify a behavior which otherwise would more nearly resemble seismic disturbances of various sorts. It is clear that more work needs to be done, preferably with our dual probe, to better categorize the nature of the acoustic emission sources.

IV. CONCLUSION

The results of this project have demonstrated the great potential of optical methods for the detection of acoustic emission. We have now an effective sensor which requires no contact with the specimen (thus does not disturb the signals) and which yields accurate, quantitative, broadband surface displacement information as well as information on disturbances in the interior of transparent materials. Optical methods have sufficient sensitivity to make the required measurements. In the laboratory we have already obtained a number of important results concerning the basic nature of acoustic emission, and we have found a method useful in the calibration of other sensors such as standard piezoelectric transducers. We are now able to make measurements at one or more points of our choosing with a sensor whose effective size is measured in microns. We can probe specimens of arbitrary size including those far too small to probe by any other technique.

Clearly much more work needs to be done on the basic nature of acoustic emission, but we now have the tools to do it. Furthermore, it seems entirely feasible to make measurements on difficult specimens such as rotating machinery and moving specimens. We can doubtless construct non-contact source location systems. Although optical methods are surely not the ultimate solution for all acoustic emissions measurements, they deserve to be a or near the top of the list of useful sensors.

REFERENCES

1. J. Kaiser, "Untersuchen über das Auftreten Gerauschen Beim Zugversuch" (Investigation of Acoustic Emission in Tensile Testing), Ph.D. thesis, Technische Hochscule, Munich, Germany (1950).
2. J. Kaiser, Ark. Eisenhüttenwessen 24, 43 (1953).
3. R. Adler, A. Korpel, and P. Desmares, IEEE Trans. Son. and Ultrasonics SU-15, 157 (1968).
4. C. H. Palmer and R. E. Green, Jr., "Optical probing of acoustic emission waves," 23rd Sagamore Army Materials Research Conference on "Nondestructive Characterization of Materials," 24-27 August (1976). (To be published).
5. A. Korpel, L. J. Laub, and H. C. Sievering, Appl. Phys. Lett. 10, 295 (1967).
6. J. Krockstad and L. D. Svaasand, Appl. Phys. Lett. 11, 155 (1967).
7. D. C. Auth and W. G. Mayer, J. Appl. Phys. 38, 5138 (1967).
8. E. P. Ippen, Proc. IEEE (Letters) 55, 248 (1967).
9. A. Alippi, A. Palma, L. Palmieri, and G. Socino, Nuovo Cimento 1 , 239 (1971).
10. R. Whitman, L. J. Laub, W. Bates, IEEE Trans. Son. and Ultrasonics SU-15, 186 (1968).
11. C. H. Palmer, R. O. Claus, and S. E. Fick, Appl. Opt. 16, 1849 (1977).
12. E. R. Peck and S. W. Obetz, J. Opt. Soc. Am. 43, 505 (1953).
13. D. Vilkomerson, Appl. Phys. Lett. 29, 183 (1976).

14. R. Mezrich, D. Vilkomerson, and K. Etzold, Appl. Opt. 15, 1499 (1976).

15. C. H. Palmer and R. E. Green, Jr., Materials Eval. 35, 107 (1977).

16. S. E. Fick and C. H. Palmer, Appl. Opt. 17, 2686 (1978).

17. N. N. Hsu, J. A. Simmons,and S. C. Hardy, Materials Evaluation 35, 100 (1977).

18. F. Breckenridge, C. Tschiegg, and M. Greenspan, J. Acoust. Soc. Am. 57, 626 (1975).

19. R. A. Kline, R. E. Green, Jr., and C. H. Palmer, J. Acoust. Soc. Am. 64, 1633 (1978).

20. L. Knopoff, J. Appl. Phys. 29, 661 (1958).

21. C. Peckeris, Proc. Nat. Acad. Sci. 41, 469 (1955).

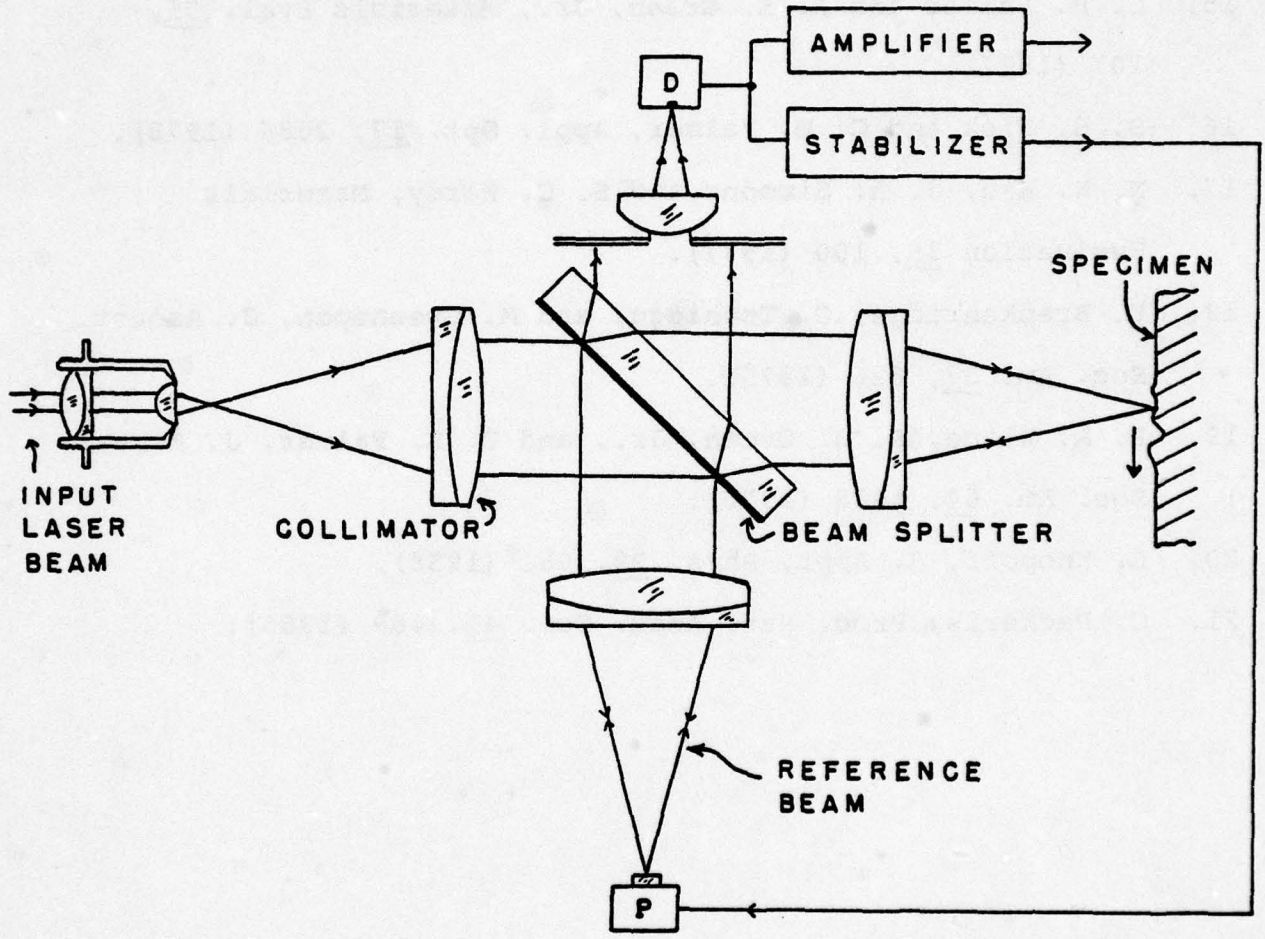

Figure II-1. Stabilized optical path interferometer. The stabilizer removes low frequency (0 to 1 kHz) disturbances; the amplifier passes the high frequency signals (> 10 kHz) which are recorded.

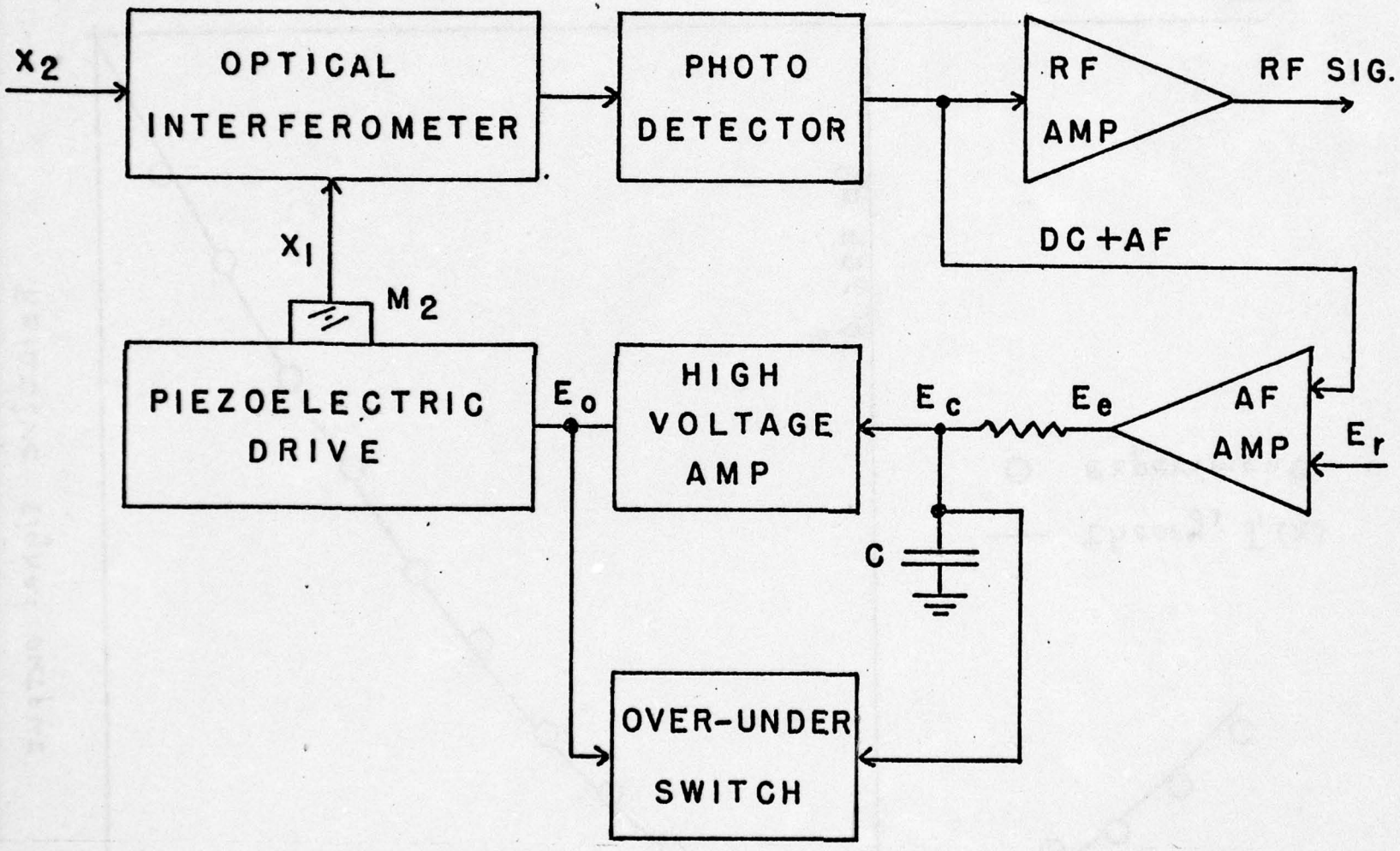

Figure II-2. Block diagram of the electronics for the stabilized path interferometer.

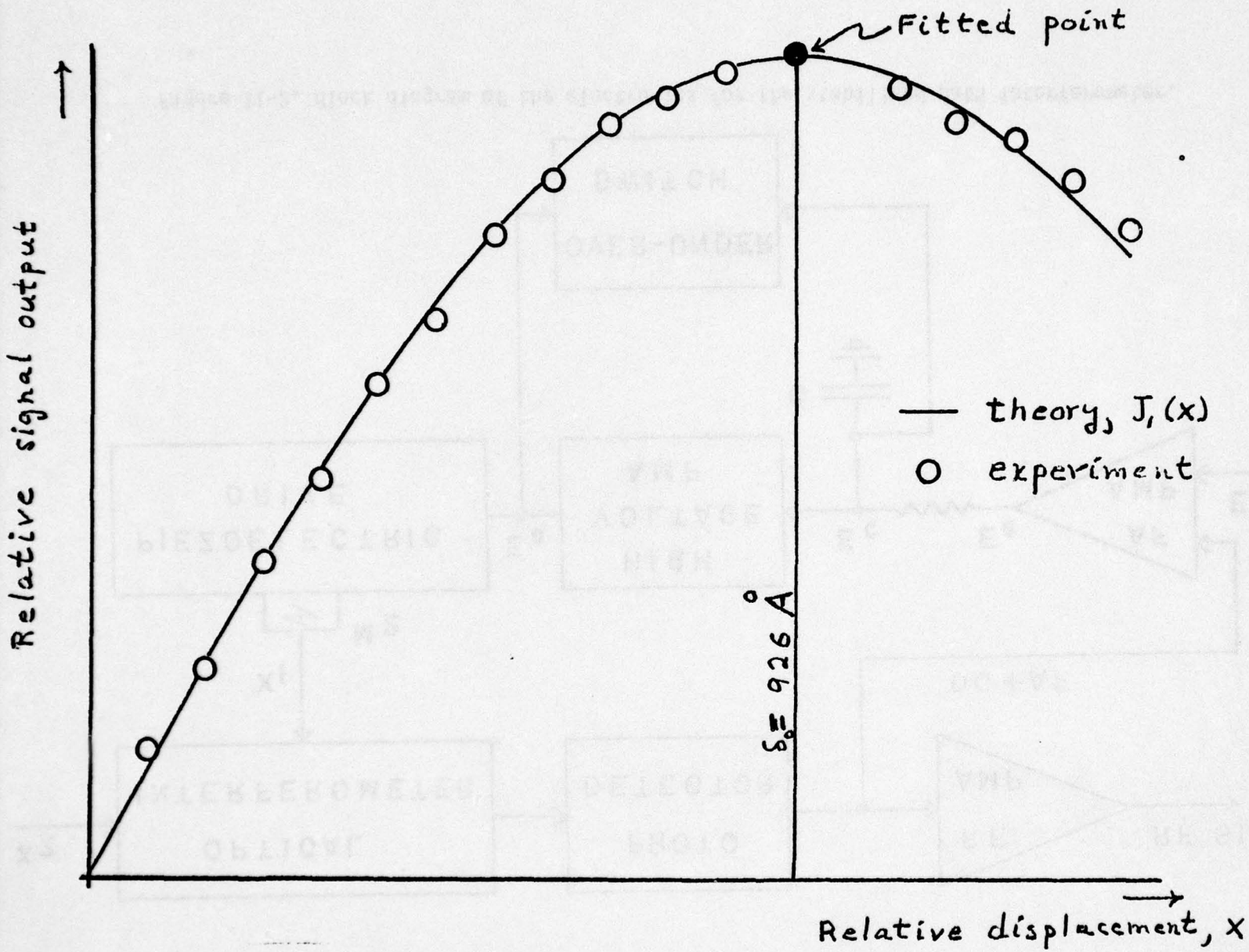

Figure II-3. Calibration curve, V_{fund} vs. displacement.

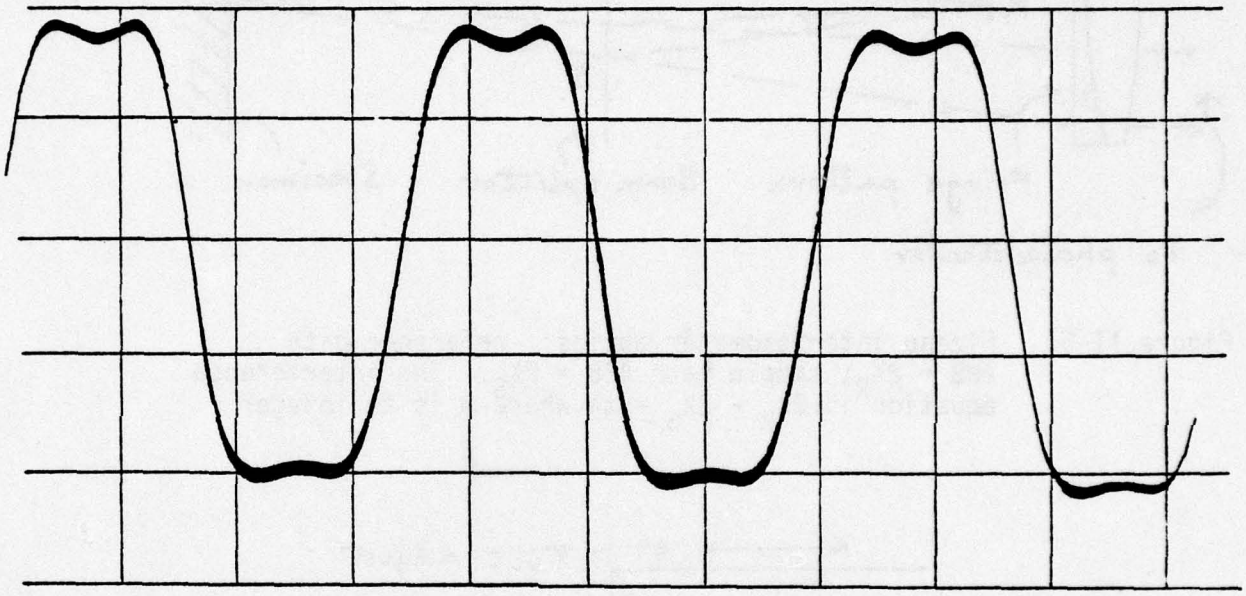

Figure II-4. Experimental calibration waveform for $\delta_o = \lambda/8 = 791$ Å. The experimental curve is indistinguishable from the theoretical curve.

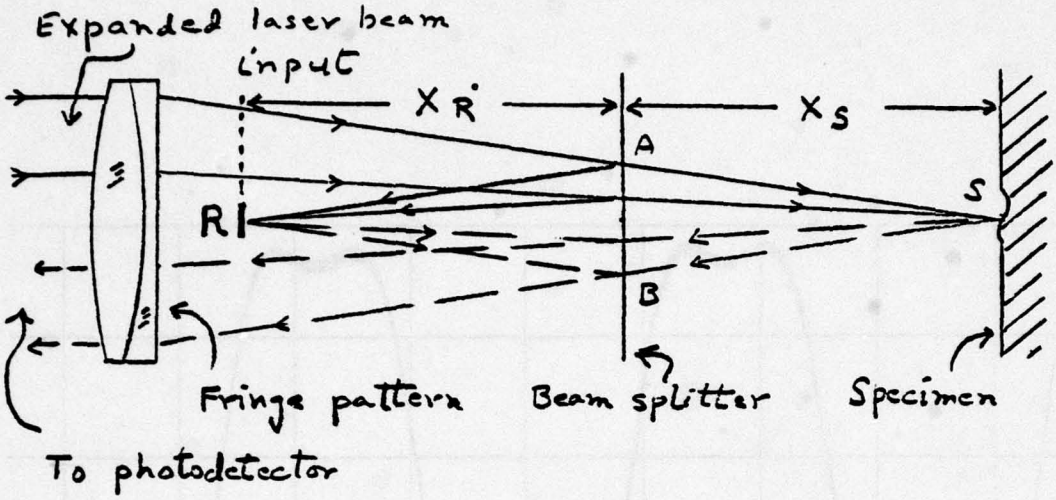

Figure II-5. Fizeau interferometer optics: reference path ARB = $2X_R$; sample path ASB = $2X_S$. The interference equation is $2X_R - 2X_S = m\lambda$ where m is an integer.

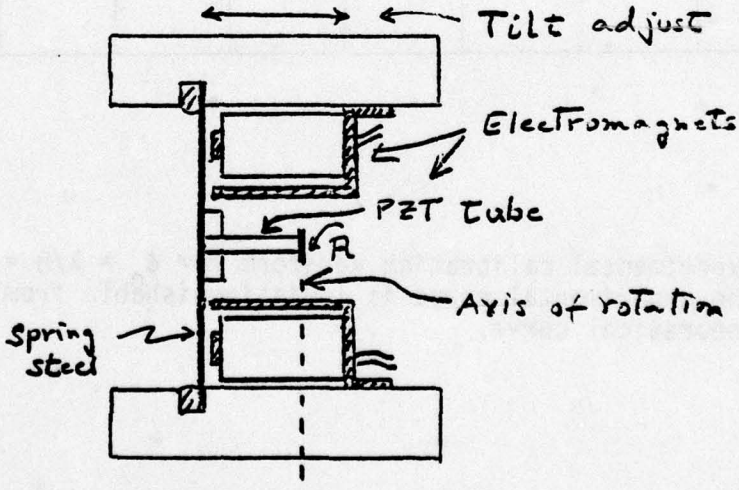

Figure II-6. Optical path correction unit. The PZT tube corrects for ~6 fringes with response time ~1msec; the electromagnets correct for ~6000 fringes with response time~100 msec.

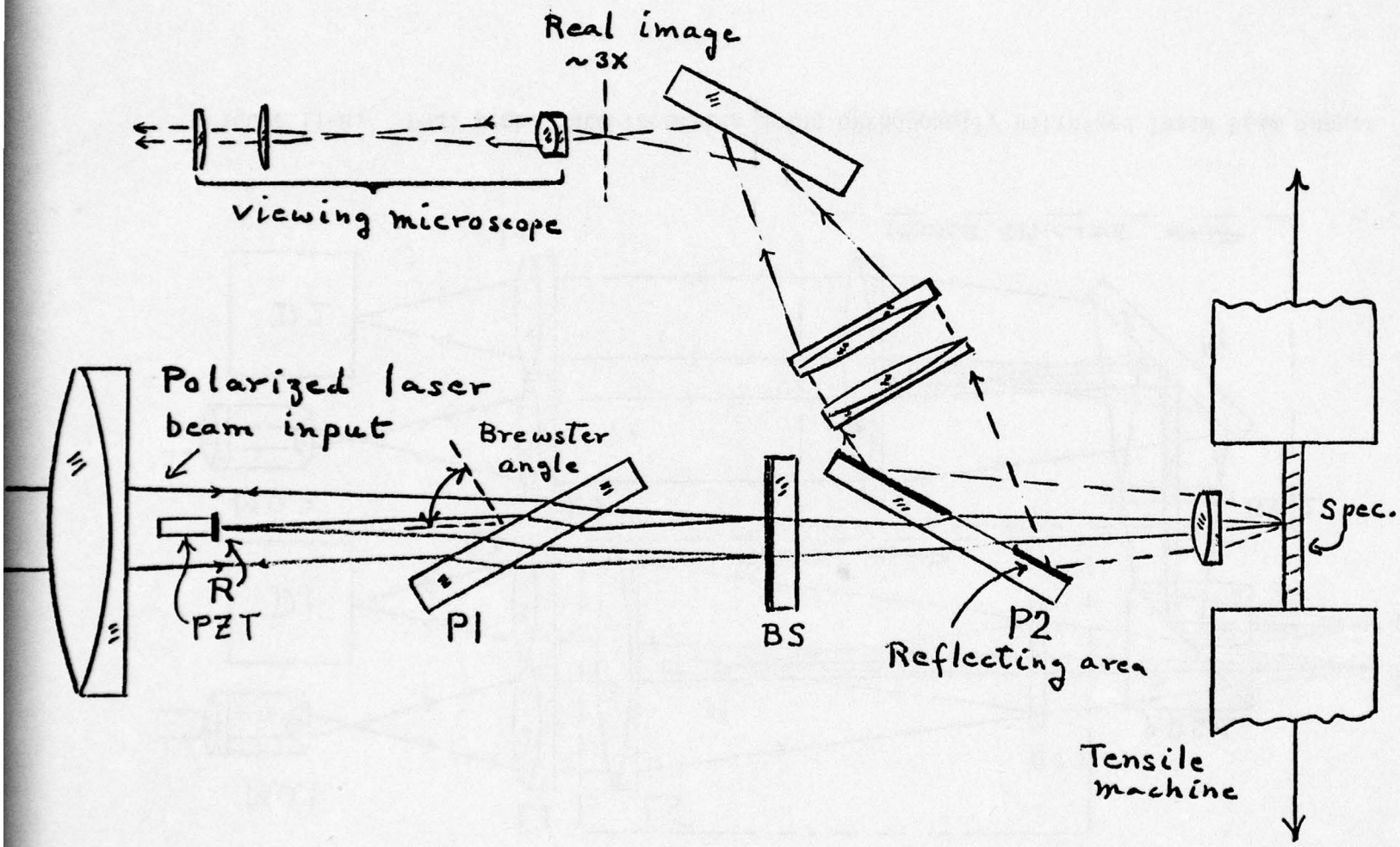

Figure II-7. Proposed viewing system for Fizeau interferometer.

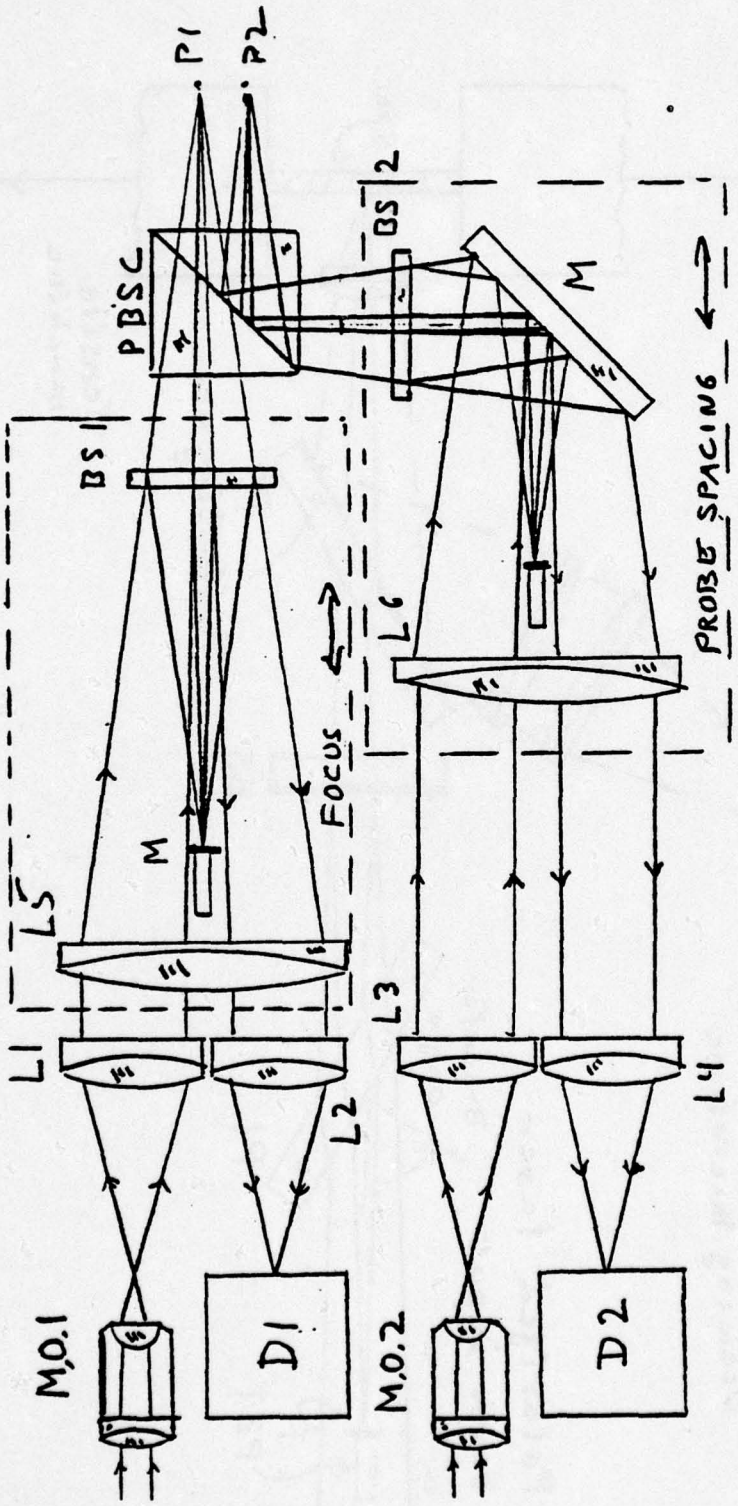

Figure II-8. Dual probe interferometer using orthogonally polarized laser beam inputs.

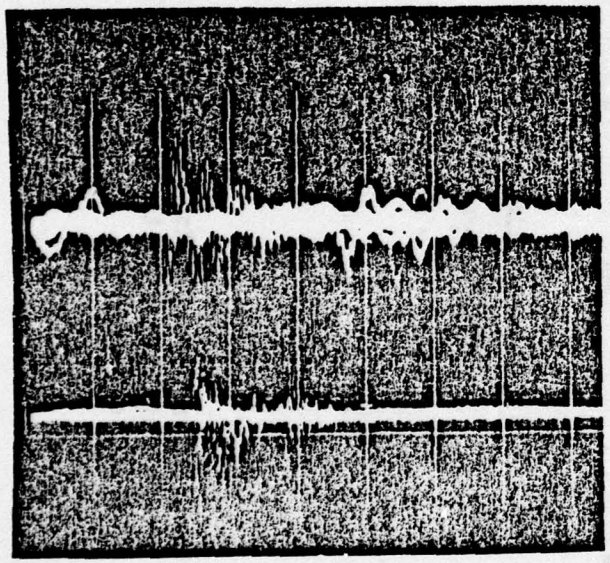

Figure II-9. One of the first optically sensed A.E. signals (above); piezoelectric comparison below. Sweep, 1 msec/div.

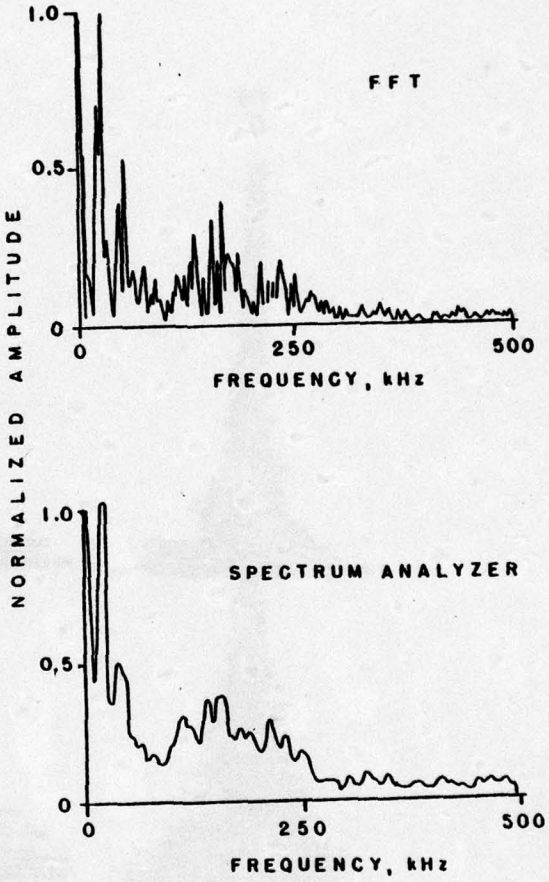

Figure II-10. Frequency spectra by FFT (above) and spectrum analyzer (below).

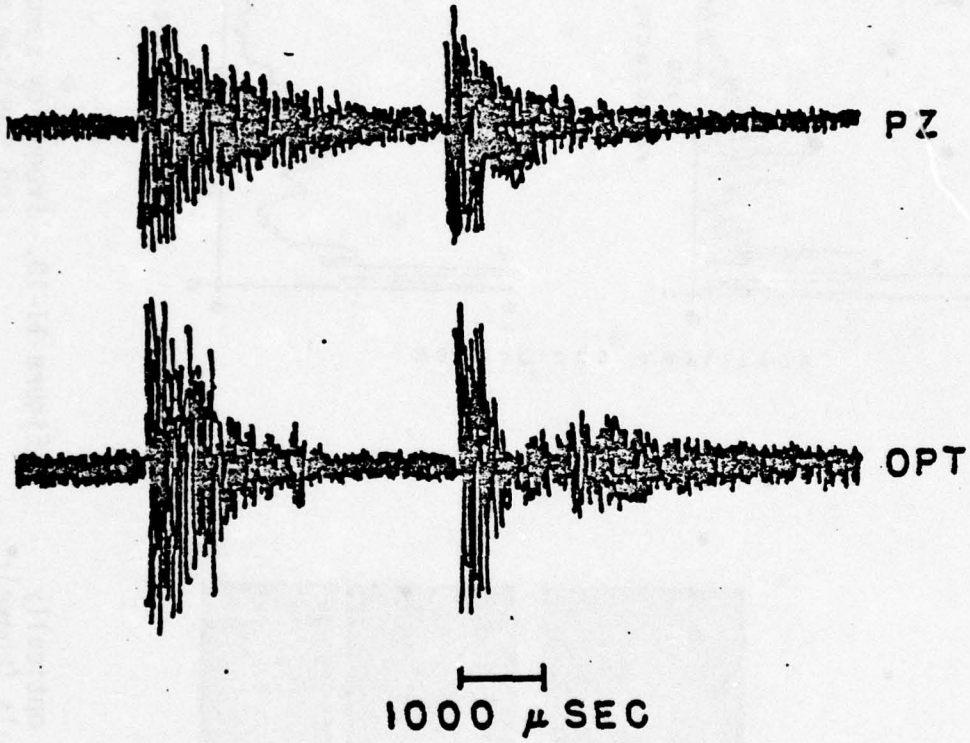

Figure III-1. Successive bursts in stress corrosion cracking in steel; upper trace piezoelectric, lower trace optical sensor.

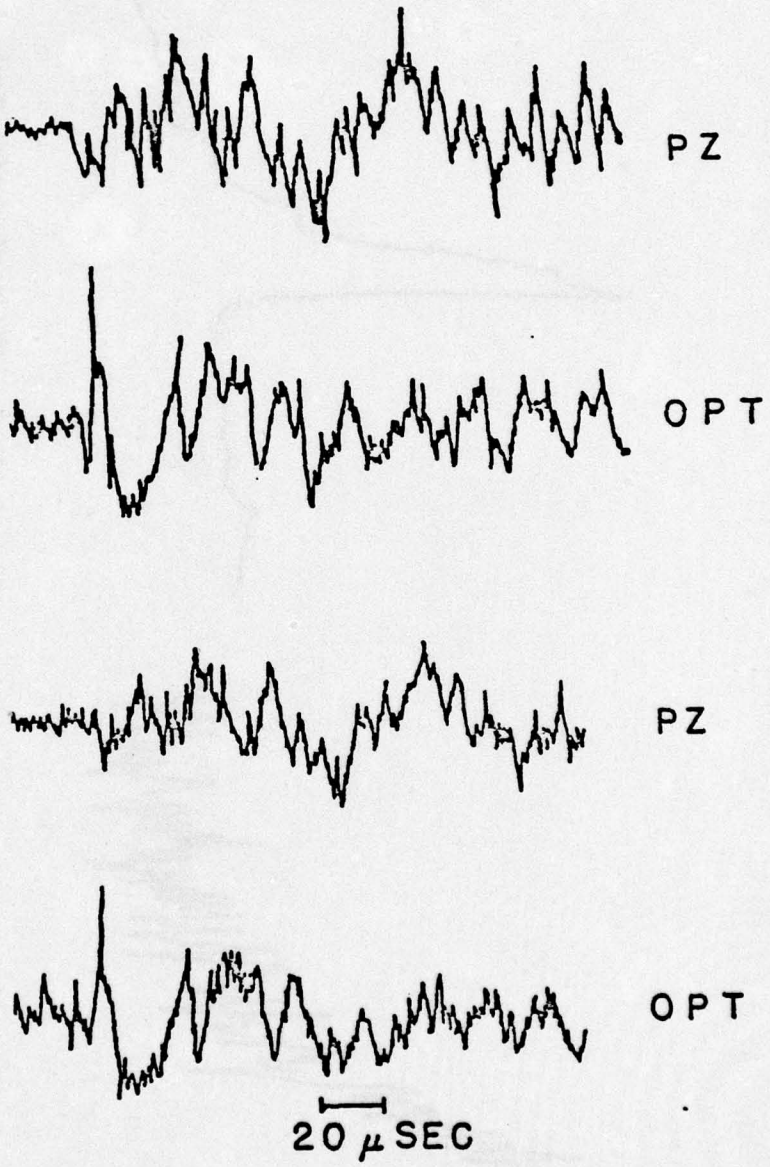

Figure III-2. Successive bursts in steel. The piezoelectric signals were obtained at the side of the specimen, the optical signals less than 1 mm from the growing crack. Note the spike in the optical signals, absent in the others.

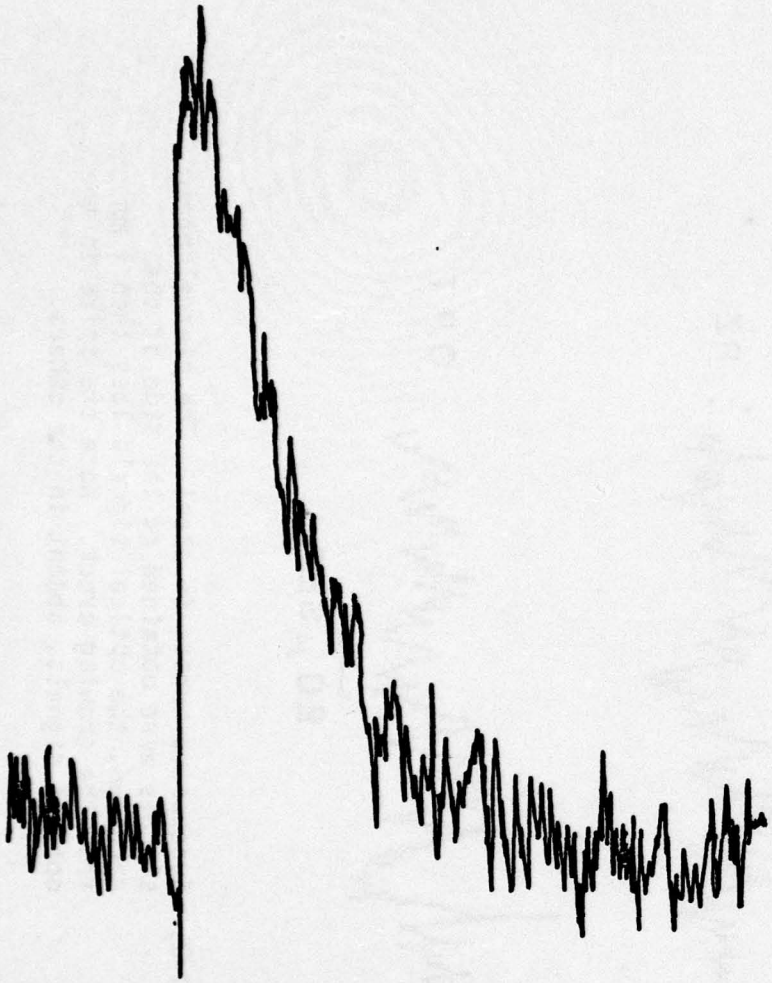

Figure III-3. Short rise time from stress-corrosion cracking in steel.

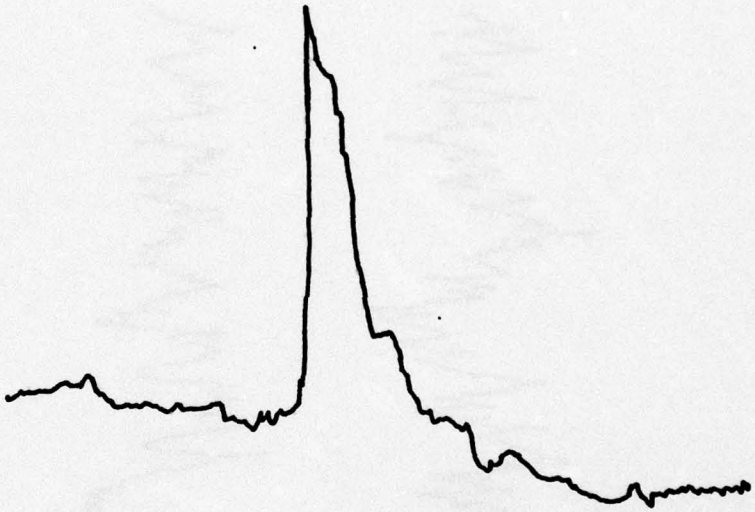

Figure III-4. Short rise time from stress-corrosion cracking in aluminum.

Figure III-5. A series of acoustic emission spikes in aluminum spaced about 40 μsec apart in time.

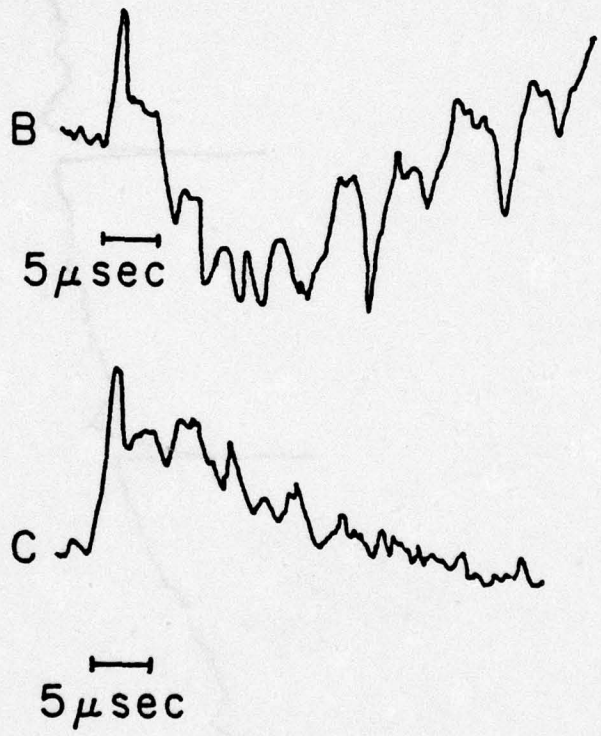

Figure III-6. Short rise times of A.E. burst in indium at -190°C measured 1 mm from source.

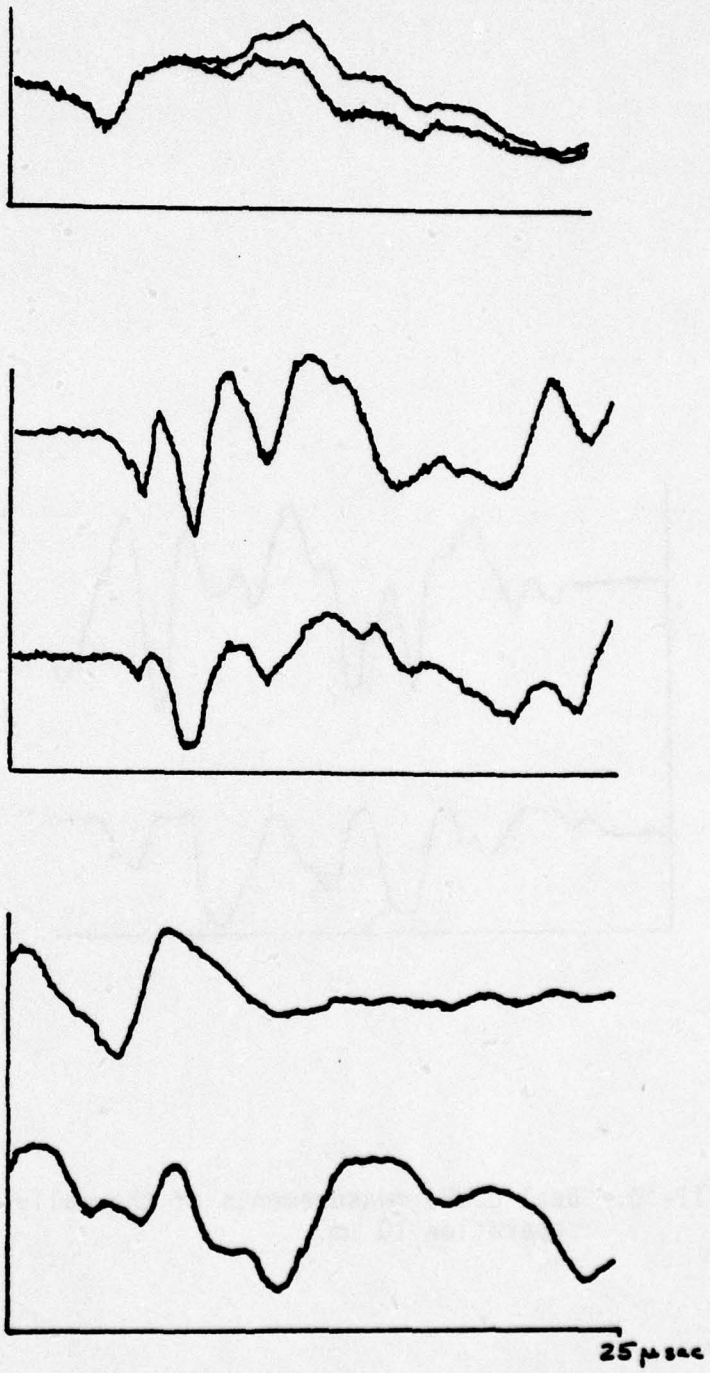

Figure III-7,8,9. Dual probe measurements of AE in steel at separations 0 mm (top), 1 mm (center), and 5 mm (bottom) showing propagational effects.

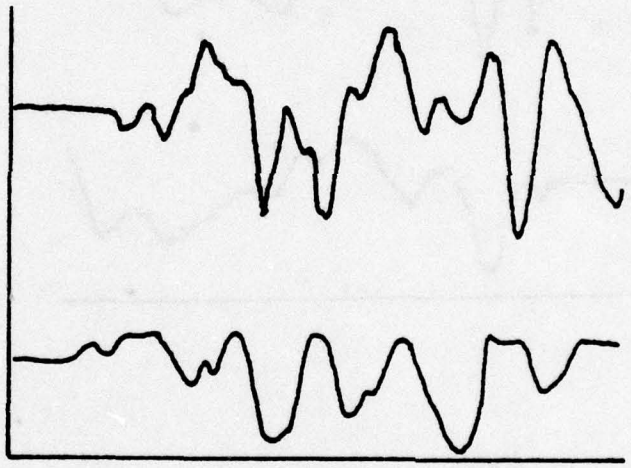

Figure III-10. Dual probe measurements of thermally cracked glass, separation 10 mm.

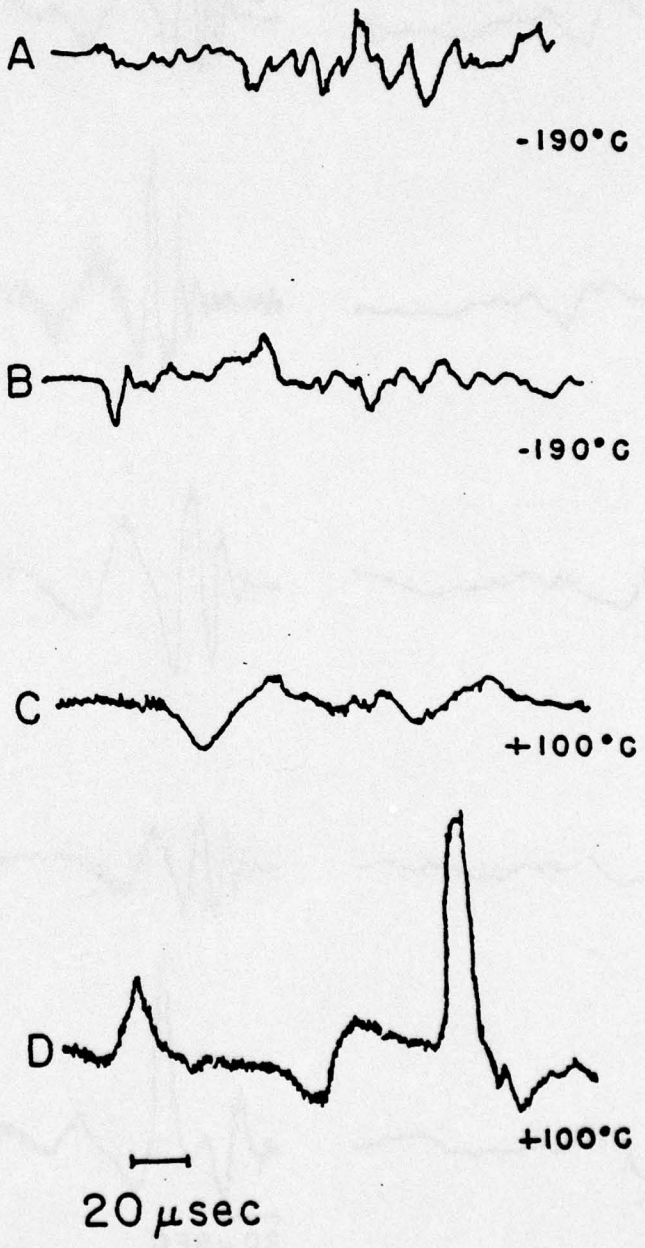

Figure III-11. Effect of temperature on twinning signals in indium. Traces A and B -190°C, traces C and D, +100°C.

Figure III-12. Characteristic acoustic emission signals. Left indium twinning (20°C); right iron phase change (900°C).

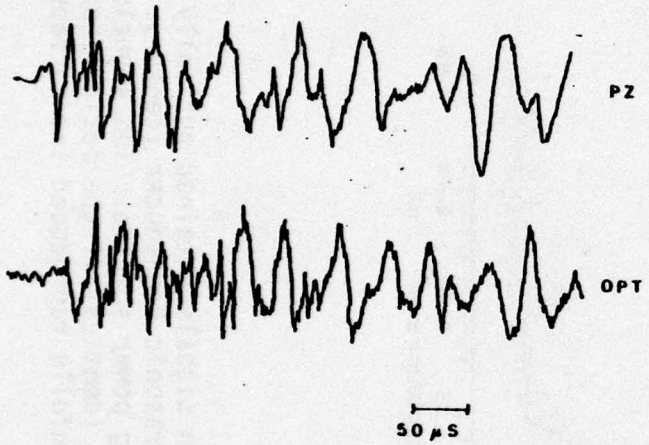

Figure III-13. Waveforms for a twinning event in indium. Piezoelectric signal (above), and optical interferometer (below).

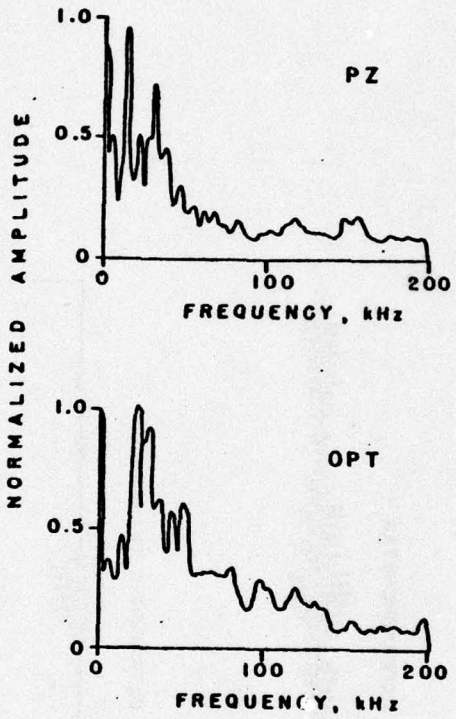

Figure III-14. Frequency spectra for the two signals of Fig. 13; upper spectrum piezoelectric, lower spectrum optical.

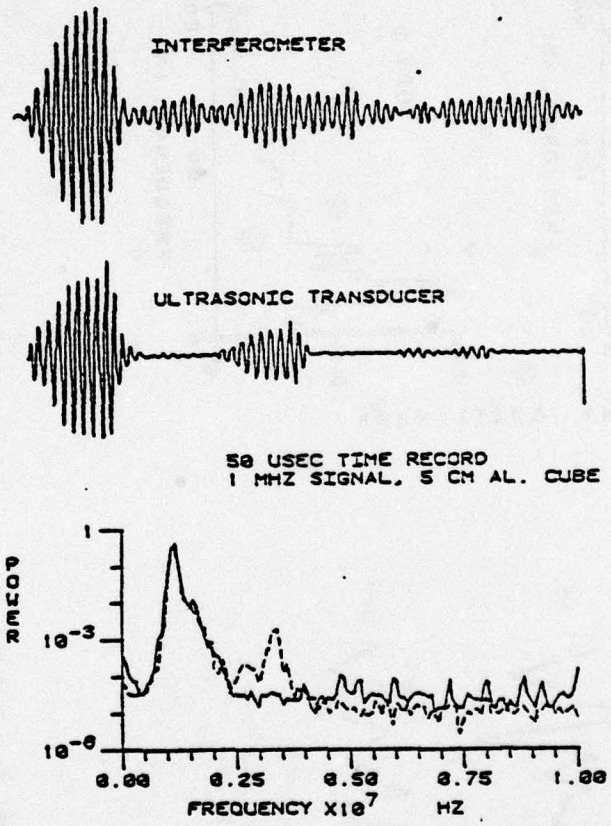

Figure III-15. Acoustic emission signals obtained optically (above) and with medical ultrasonic transducer (center). Below are the corresponding power spectra. The signals and their spectra would be identical if the optical and ultrasonic transducers faithfully reproduced the surface displacements.

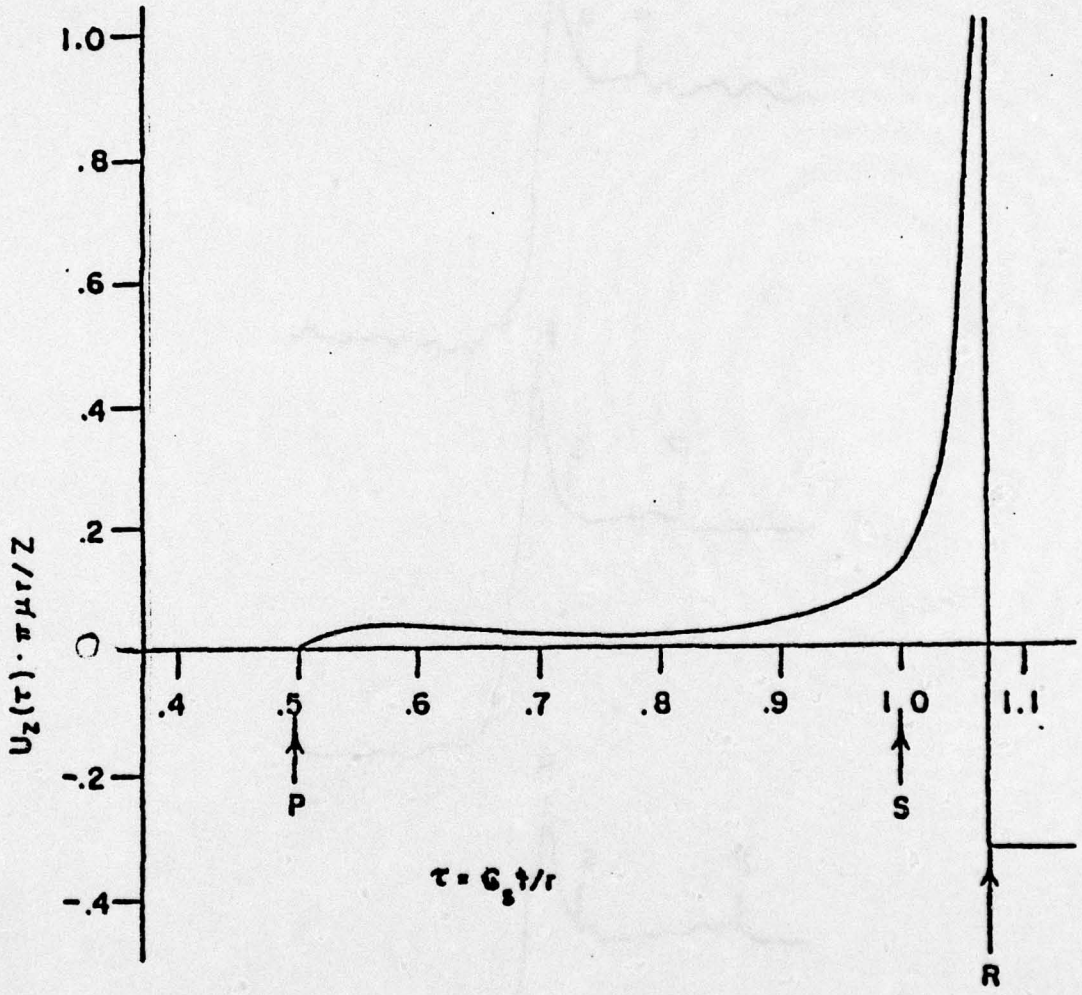

Figure III-16. Theoretical surface displacement for a seismic surface pulse.

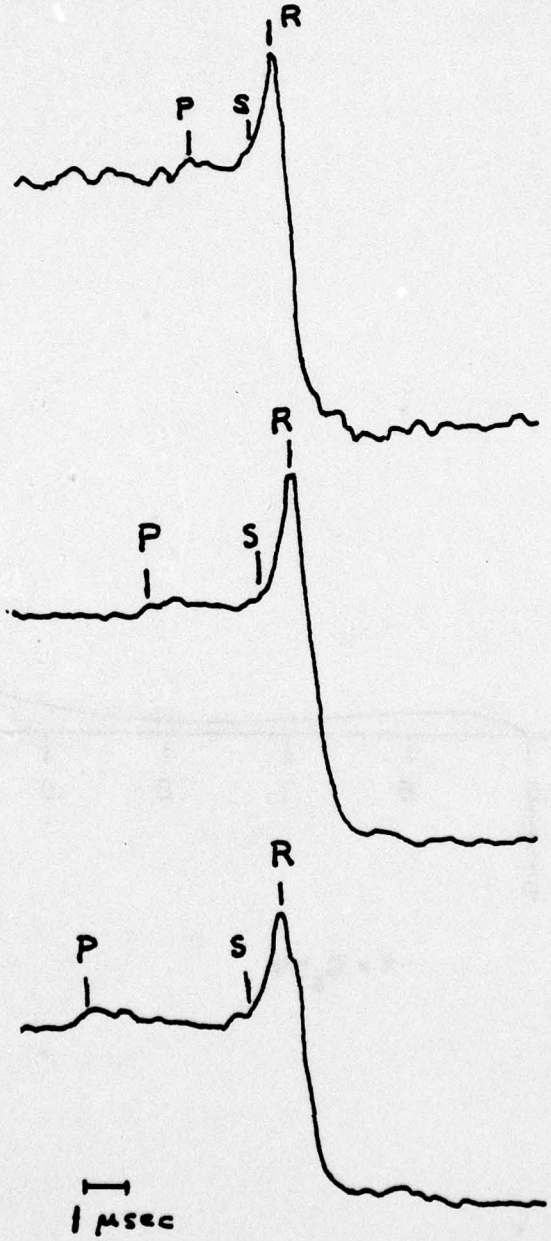

Figures 17,18,19. Measured surface displacements for seismic surface pulses at distances 10 mm (top), 20 mm (center), and 30 mm (bottom) from the source, respectively.

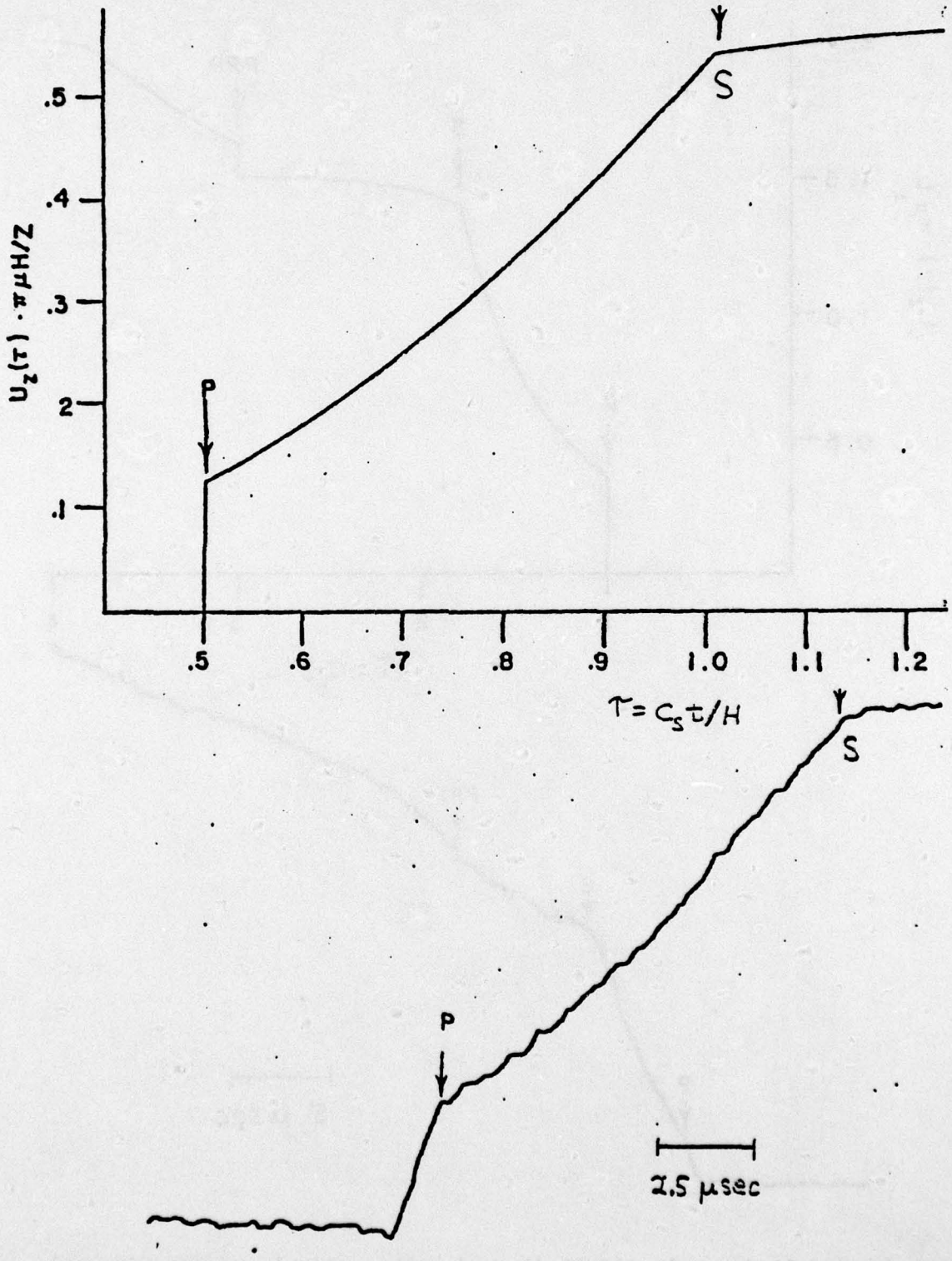

Figures III-20 (upper), III-21 (lower). Theoretical and experimental surface displacement for seismic buried pulse.

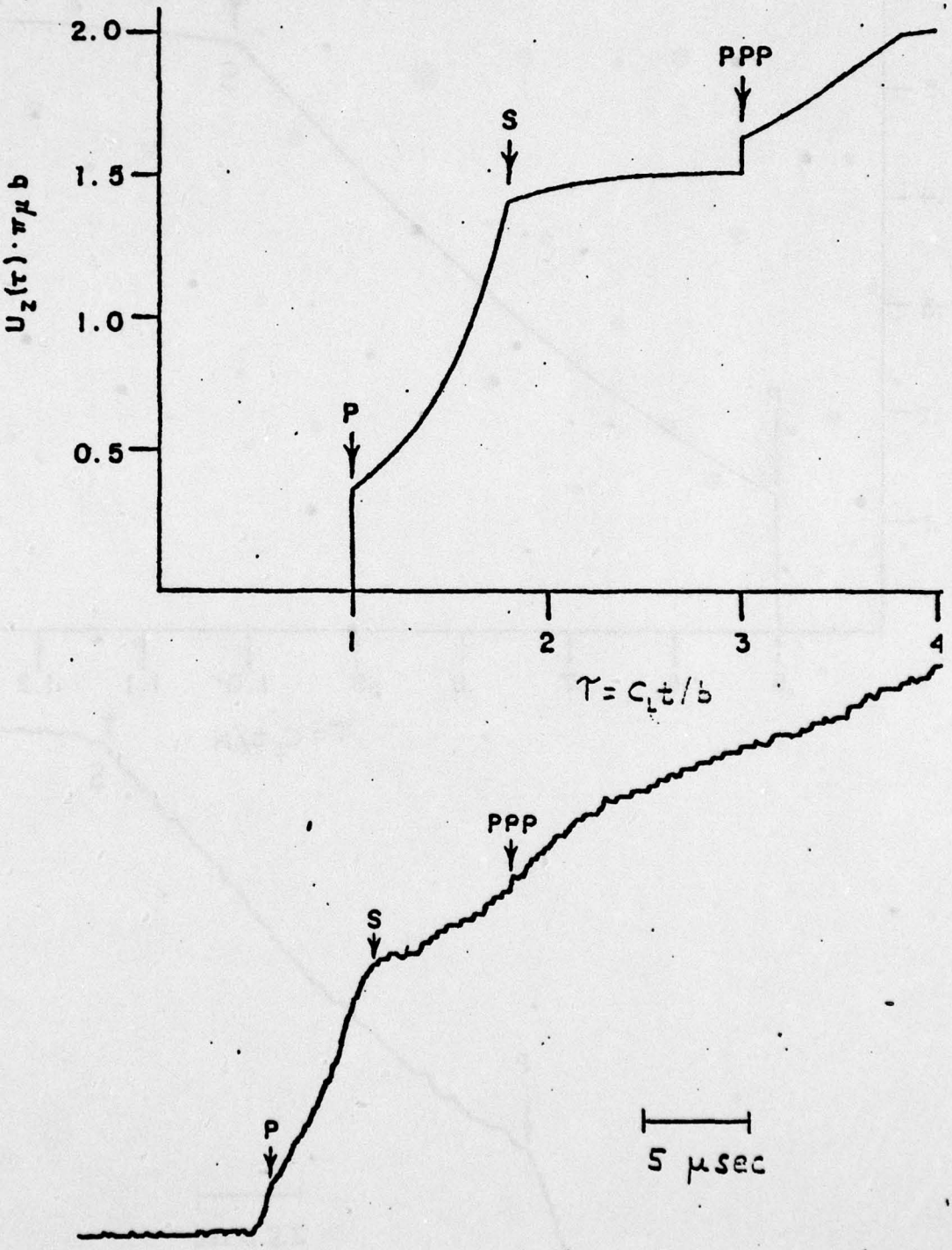

Figures III-22 (upper), III-23 (lower). Theoretical and experimental surface displacement for thick slab experiment.

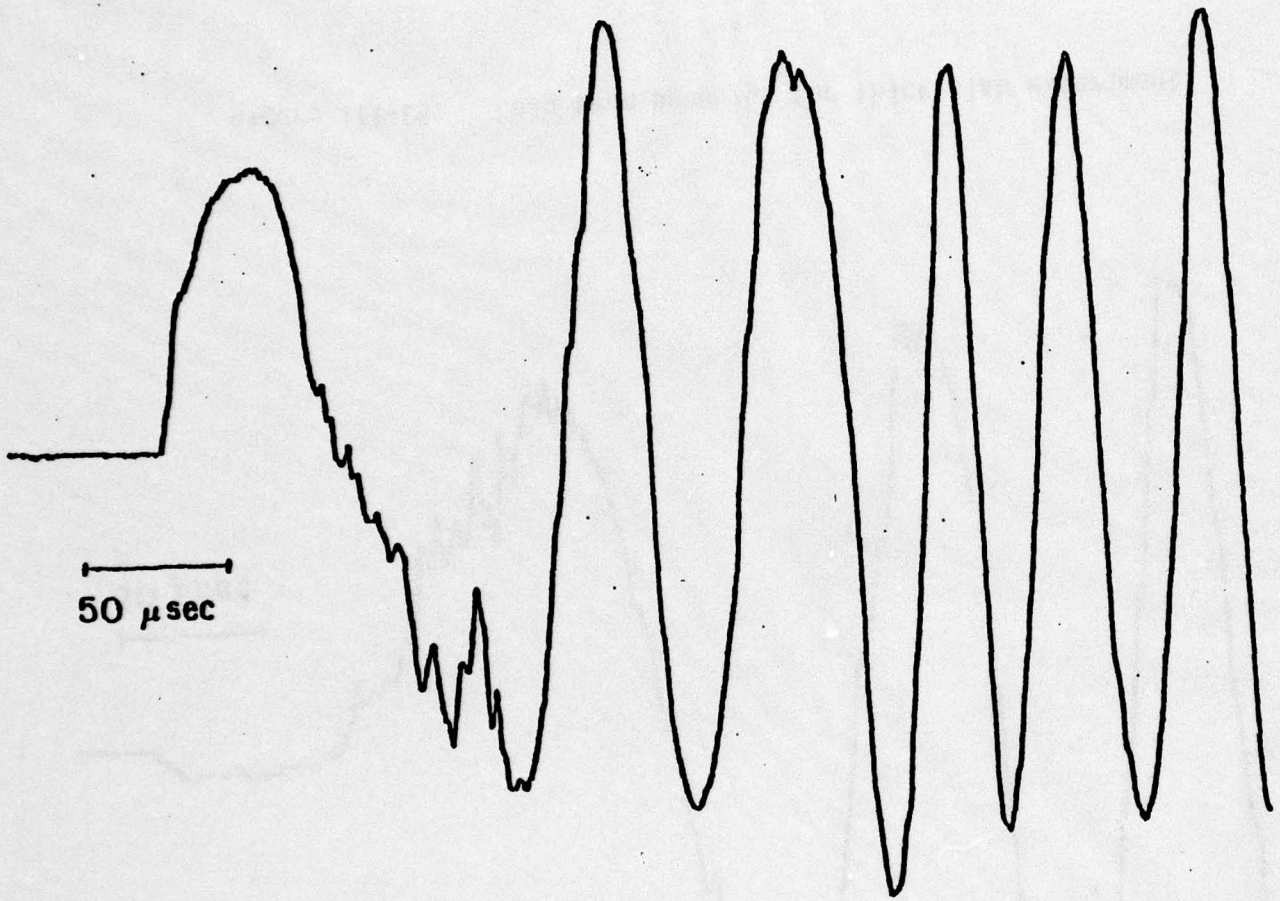

Figure III-24. Long term behavior for seismic buried pulse experiment.

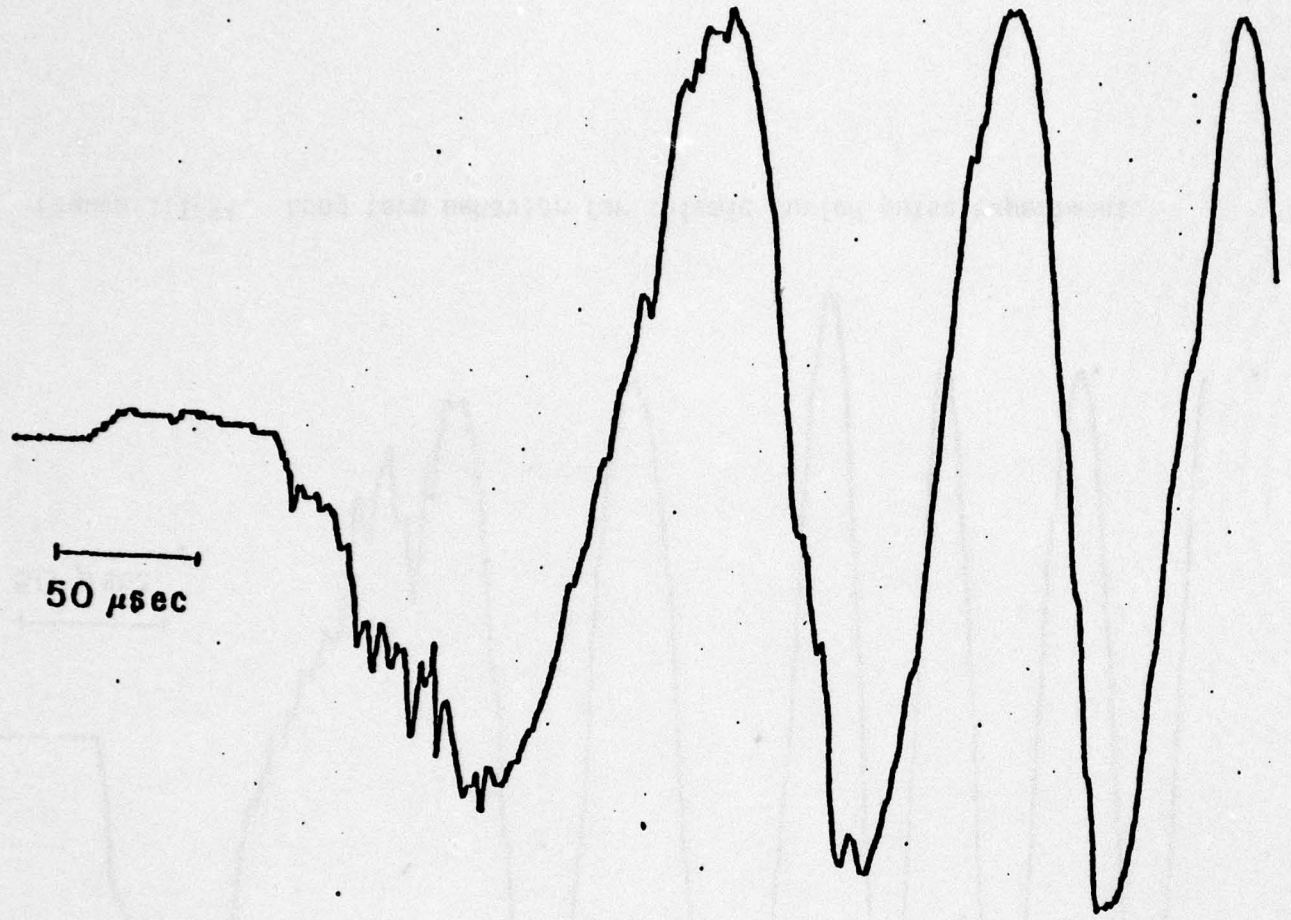

Figure III-25. Long term behavior for thick slab experiment.

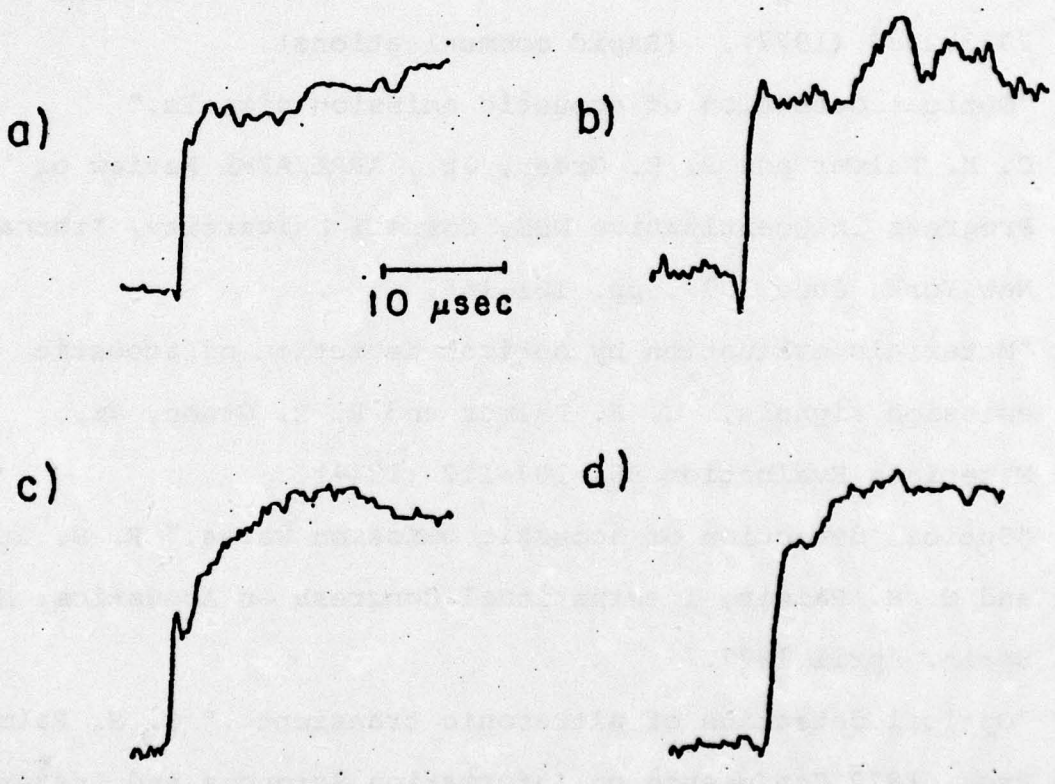

Figure III-26. Typical acoustic emission bursts from steel measured near the crack. Note the short rise time and similarity to seismic sources.

PUBLICATIONS DIRECTLY RESULTING FROM GRANTS

1. "Optical probing of acoustic emission waves," C. H. Palmer and R. E. Green, Jr., 23rd Sagamore Army Materials Research Conference on "Nondestructive Characterization of Materials," 24-27 August 1976. (To be published).
2. "Optical detection of acoustic emission waves," C. H. Palmer and R. E. Green, Jr., Applied Optics, 16, 2333-2334 (1977). (Rapid communications).
3. "Optical detection of acoustic emission signals," C. H. Palmer and R. E. Green, Jr., ARPA/AFML Review of Progress in Quantitative NDE, Cornell University, Ithaca, New York, June 1977, pp. 161-165.
4. "Materials evaluation by optical detection of acoustic emission signals," C. H. Palmer and R. E. Green, Jr., Materials Evaluation 35, 107-112 (1977).
5. "Optical detection of acoustic emission waves," R. E. Green, Jr. and C. H. Palmer, International Congress on Acoustics, Madrid, Spain, April 1977.
6. "Optical detection of ultrasonic transients," C. H. Palmer, Proc. 1978 Conference on Information Sciences and Systems, Johns Hopkins University, Baltimore, Maryland, 1978, pp. 559-563.
7. "A comparison of optically and piezoelectrically sensed acoustic emission signals," R. A. Kline, R. E. Green, Jr., and C. H. Palmer, J. Acoust. Soc. Am. 64, 1633-1639 (1978).

8. "Optical and Piezoelectric Detection of Acoustic Emission Signals," R. A. Kline, Ph.D. Thesis, Baltimore, 1978.

9. "The measurement and generation of ultrasound by lasers," C. H. Palmer, Proc. First International Symposium on Ultrasonic Materials Characterization, National Bureau of Standards, 7-9 June 1978.

10. "Visualization of ultrasonic bulk waves in solids with an internal light probe," B. B. Djordjevic and R. E. Green,Jr., Proc. First International Symposium on Ultrasonic Materials Characterization, National Bureau of Standards, 7-9 June, 1978.

11. "Optical measurement of acoustic emission at high and low temperatures," C. H. Palmer, ARPA/AFML Review of Progress in Quantitative NDE, San Diego, California, July 1978, pp. 437-440.

12. "New optical instrument for acoustic emission," C. H. Palmer and S. E. Fick, IEEE Southeastcon, Roanoke, Virginia, April 1979, pp. 191-192.

13. "Laser beam detection of ultrasonic and acoustic emission signals for nondestructive testing of materials," R. E. Green, Jr., B. B. Djordjevic, C. H. Palmer, and S. E. Fick, National Symposium on "Applications of Lasers to Materials Processing". (To be published).

14. "High speed digital capture of acoustic emission and ultrasonic transients as detected with optical laser beam probes," B. B. Djordjevic and R. E. Green, Jr., Ultrasonics International 79 Conference, Graz, Austria, May 1979.

15. "Real and simulated acoustic emission from stress corrosion cracking in steel," R. A. Kline, R. E. Green, Jr., and C. H. Palmer, (In preparation).

OTHER PUBLICATIONS INDIRECTLY RELATED TO GRANT

1. "Ultrasonic Wave Measurement by Differential Interferometry," C. H. Palmer, R. O. Claus, and S. E. Fick, Appl. Opt. 16, 1849 (1977).
2. "The Optical Measurement of Ultrasonic Stoneley Waves," R. O. Claus, Ph.D. Tesis, Baltimore, June 1977.
3. "Direct Measurement of Ultrasonic Stoneley Waves," R. O. Claus and C. H. Palmer, Appl. Phys. Lett. 31, 547 (1977). (Letter).
4. "Three Dimensional Measurements of Ultrasonic Waves in Solids," S. E. Fick, Ph.D. Thesis, Baltimore, June 1978.
5. "Three Dimensional Real Time Measurements of Ultrasonic Waves in Transparent Solids," Appl. Opt. 17, 2686 (1978). (Letter).

Scientific Personnel supported in whole or in part by these grants and degrees awarded during the period 2/15/76 through 6/30/79.

C.Harvey Palmer, Co-Principal Investigator, Professor, Electrical Engineering (Joint Appointment in Materials Science and Engineering).

Robert E. Green, Jr., Co-Principal Invesitgator, Professor, Materials Science and Engineering.

Steven E. Fick, Post Doctoral Student, Ph.D., Electrical Engineering, June 1978.

Richard O. Claus, Graduate student, Ph.D., Electrical Engineering, June 1977.

Ronald A. Kline, Graduate student, Ph.D., Mechanics and Materials Science, June 1977. (No support)

B. Boro Djordjevic, Graduate student, Materials Science and Engineering.

Equipment Loans

We are grateful for the loan of several major pieces of auxilrary equipment used for this project.

Dr. Richard O. Claus, Virginia Polytechnic and State University,
--HeNe laser

Dr. Robert W. Penn, National Bureau of Standards,
--Video tape recorder

Dr. Richard D. Deslattes, National Bureau of Standards,
--HeNe laser

Mr. Gary Brown, Representative of Nicolet Corp.,
--Nicolet Explorer Oscilloscope.